

# SoK: Cryptographic Protection of Random Access Memory

Roberto Avanzi<sup>1,2</sup>, Andreas Sandberg<sup>3</sup>, Ionuț Mihalcea<sup>3</sup>,  
David Schall<sup>4</sup> and Héctor Montaner<sup>5</sup>

<sup>1</sup> Arm Germany GmbH, Grasbrunn, Germany

[roberto.avanzi@arm.com](mailto:roberto.avanzi@arm.com)

<sup>2</sup> Caesarea Rothschild Institute, University of Haifa, Israel

[roberto.avanzi@gmail.com](mailto:roberto.avanzi@gmail.com)

<sup>3</sup> Arm Limited, Cambridge, United Kingdom

[{andreas.sandberg, ionut.mihalcea}@arm.com](mailto:{andreas.sandberg, ionut.mihalcea}@arm.com)

<sup>4</sup> School of Informatics, University of Edinburgh, United Kingdom

[david.schall@ed.ac.uk](mailto:david.schall@ed.ac.uk)

<sup>5</sup> Graphcore, Cambridge, United Kingdom

[hector.montaner@outlook.com](mailto:hector.montaner@outlook.com)

**Abstract.** Confidential Computing is the protection of data in use from access or modification by any unauthorized agent, including privileged software. For example, in Intel SGX and TDX, AMD SEV, and Arm CCA this protection is implemented via access control policies. Some of these architectures also include memory protection schemes relying on cryptography, to protect against physical attacks.

We review and classify such schemes, from academia and industry, according to the offered protection levels. The protection levels in turn depend on models of adversaries with varying capabilities, budget, and strategy.

The building blocks of all memory protection schemes are encryption and integrity primitives, and anti-replay structures. We review these building blocks, consider their possible combinations, and evaluate the performance impact of the resulting schemes.

We present a framework for the performance evaluation in a simulated system. To understand the best and worst case overhead, systems with varying load levels are considered.

We propose new solutions to further reduce the performance and memory overheads of such technologies. We show that advanced counter compression techniques make it viable to store counters used for replay protection in a physically protected memory. By repurposing some ECC bits to store integrity tags, we achieve hitherto unattained performance while providing confidentiality, integrity, and replay protection.

**Keywords:** Security and privacy · Hardware-based security protocols · Memory Encryption · Memory Integrity · Lightweight ciphers · Integrity Trees

## 1 Introduction

Cloud computing promises to increase efficiency and drive down cost for users. Such services co-locate multiple mutually untrusted tenants in the same data center and sometimes even on the same physical machines. Compared to traditional on-premises solutions, users of cloud computing face two additional threats. First, hostile tenants may try to exploit bugs in the hypervisor or *access control* mechanisms to impact the confidentiality,

integrity, or availability of co-located virtual machines. Second, compromised insiders at the service provider or its contractors may try to gain access to customer data.

Similar threats exist in client devices, such as phones, which have evolved into smart terminals and identity providers. Like in a data center, adversaries may use co-located untrusted code or even have physical access to the device. Use cases such as secure payments, secure identification, and software anti-piracy rely on strong confidentiality and integrity guarantees. These are often provided in separate components, e.g., SIM cards, USB tokens, or *Trusted Platform Modules (TPMs)*. Consolidating their functionality onto the main *System-on-a-Chip (SoC)* enables new use cases while reducing total costs — but also enables opportunities for the aforementioned adversaries.

AMD SEV [KPW16], Arm CCA [MPS<sup>+</sup>21], Intel’s Client SGX [Gue16a] and Scalable SGX [JMSS20], and Intel TDX [Int21] move towards this goal by providing access control mechanisms. The latter are managed by a HW-supported *Trusted Computing Base (TCB)*. Some of these technologies even include protection against adversaries with physical access to the system. For instance, Intel’s Client SGX implements a *Memory Encryption Engine (MEE)* [Gue16a] that provides confidentiality, as well as integrity and protection against replay attacks. Such strong security guarantees can be very costly in terms of performance and storage. For this reason, AMD SEV, Intel TDX, and Scalable SGX (the latter two sharing the same memory protection scheme) provide weaker guarantees in exchange for better performance.

**The question that we answer in this study is: *What cryptographic technologies are available to protect the contents of data-in-use in RAM against an adversary with physical access to the system, and what are their memory overheads and performance costs?***

The starting point is a thorough review of the techniques documented in the scientific and technical literature. Even though we cite several architectures for implementing complete *Trusted Execution Environments (TEEs)*, the scope of this paper does not address aspects such as *Operating System (OS)* and Hypervisor support, I/O, virtualization, attestation and IPC mechanisms. We focus on solutions for cryptographic memory protection that are entirely implemented within the SoC package limits.

In real-world applications, understanding the cost of a solution is crucial. Area and power constraints limit the viable options, but relaxing them can be justified by strong market requirements. On the other hand, solutions with high performance penalties and memory overheads risk being rejected without further consideration of their merits. For this reason, we compare the costs of several schemes and variations thereof, where *we focus mainly on performance penalty and memory overheads*. We also propose new methods to further reduce these costs.

Our performance evaluation uses the entire industry-standard SPEC 2017 [BLvK18] benchmark suite running on the gem5 simulator [BBB<sup>+</sup>11, LAA<sup>+</sup>20].

This work also fills a gap in the literature, as there are only very few papers surveying the subject. The 2009 paper [ECG<sup>+</sup>09] is a survey of memory integrity schemes, intended as *full integrity*, i.e., including replay protection. The 2013 paper [HT13] contains a thorough survey of memory encryption techniques until its publication, but its performance data is taken from the surveyed papers, which more often than not cannot be properly compared to each other. Its abstract states “*To date, little practical experimentation has been conducted, and the improvements in security and associated performance degradation has yet to be quantified.*” Ten years later, this sentence still holds true. The more recent papers [Shw15, MZLS18, SNR<sup>+</sup>18a, TSB18, TBC<sup>+</sup>20, SNOT21, SA21, IMO<sup>+</sup>22] compare only very few schemes to each other.

**Outline of the paper.** We start with a summary of the contributions in Section 2. Following this, Section 3 contains background material, such as: the models of the adver-

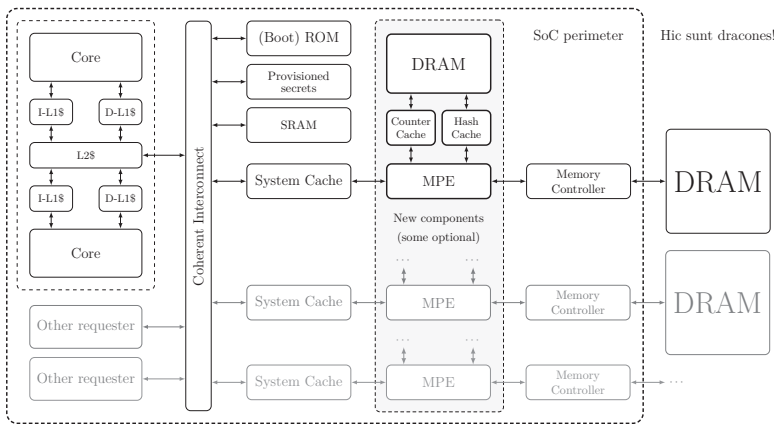


**Figure 1:** Simplified system level view of a SoC with Memory Protection Engine(s).

saries and a discussion of the memory protection levels. Section 4 contains a review of the cryptographic primitives and memory integrity structures; as well as a discussion of cryptographic parameters such as key and MAC lengths. Section 5 describes the actual benchmarks and discusses how these support the claims in Section 2. In Section 6 we conclude.

## 2 Summary of the Results

Cryptographic memory protection relies on:

- (i) Encryption,
- (ii) Authentication, and
- (iii) Replay protection structures.

In the third group we also include the protection of *a relatively small amount of* RAM, such as placing it on-chip, or in a tamper-proof or -evident device with a secured communication channel to the SoC. We exclude applying this approach to the entire RAM, because cost and thermal considerations would make it impractical for general use.

There are only a few meaningful combinations of these technologies. They are added sequentially to access control, forming four increasingly robust *Protection Levels*:

- L0: Access Control only;
- L1: L0 + Memory encryption;
- L2: L1 + Memory integrity; and
- L3: L2 + Protection against replay attacks.

While one can imagine use cases for various degrees of integrity protection only without encryption, we are not aware of any such scheme.

We implement Protection Levels L1 to L3 in the *Memory Protection Engine (MPE)*, an IP block sometimes known as *Memory Encryption Engine (MEE)*, e.g., in SGX. As depicted in Fig. 1, in a typical SoC the MPE sits between the main interconnect (or a system cache) and a memory controller. It can optionally have its own caches, and even access to a physically secure private DRAM to store metadata.

Table 1: Selected documented TEEs and cryptographic memory protection schemes.

System	Year	Level	AC	Encryption	Authentication	Structure	References
Hall and Jutila's PAT	2002	L3	N	Unspecified	Unspecified	Counter Tree	[HJ08]
ABEGIS	2003	L3	N	AES-CBC	Incremental hash	<i>Merkle Tree (MT)</i>	[SCG <sup>+</sup> 03a, GSC <sup>+</sup> 03]
ABEGIS (alt. design)	2003	L3	N	"OTP"	MD5/SHA-1	Log Hashes	[SCG <sup>+</sup> 03b]
Yan et al.	2006	L3	N	AES-GCM	GMAC	Split Counter Tree	[YEP <sup>+</sup> 06]
SecureMe	2007	L3	N	AES-CTR	SHA-1/HMAC	Bonsai MT	[RCP807]
Bastion	2010	L3	Y	AES-ECB	AES-CMAC	MT	[CL10]
IVEC	2010	L3	N/A	AES-GCM	GMAC	Split Counter Tree, MACs in ECC bits	[HS10]
SecureBlue++	2011	L3	N	Unspecified	Unspecified	"Integrity tree"	[WB11]
H-SVM	2011	L0	Y	None	None	Managed page tables	[JACH11]
Hyperwall	2011	L0	Y	None	None	Verified page tables	[SL12]
Bloom Filters	2012	L3	N/A	N/A	Bloom Filter	Hash Tree	[NHSQ12]
Intel's Client SGX1/SGX2	2013	L3	Y	AES-CTR	Encrypted UHF	Counter Tree	[MAR <sup>+</sup> 13]
Iso-X	2014	L0	Y	Optional	Optional	Optional	[EEO <sup>+</sup> 14]
PodArch	2015	L3	Y	AES-GCM	GMAC	On-demand secure encryption	[Shw15]
AMID-SEV-SNP	2016	L1	Y	AES-XEX	None	None	[AMID20b, KPW16, AMID20a]
SYNERGY	2018	L3	N/A	AES-GCM	GMAC	Bonsai MT, MACs in ECC bits	[SNR <sup>+</sup> 18b]
VAULT	2018	L3	N/A	Unspecified	Unspecified	Variable-arity tree, with encrypted leaves without MACs	[TSB18]
TIMBER-V	2019	L0	Y	None	None	None	[WWB <sup>+</sup> 19]
Apple's Secure Enclave	2020	L3	Y	AES-XEX	AES-based CMAC	Bonsai "Integrity tree"	[App20]
Intel TDX, Scalable SGX	2020	L2	Y	AES-XEX	Reduced SHA-3	MACs in ECC bits	[Int21, JMSS20]
Keystone	2020	L1-L3	Y	AES-128, in an unspecified mode	Unspecified	Secure paging of on-chip memory to external RAM	[LKS <sup>+</sup> 20]
Arm CCA	2021	L0	Y	Optional	Optional	Optional	[MPS <sup>+</sup> 21]
PENGLAI	2021	L3	Y	Unspecified	Unspecified	Dynamically allocated MT	[FLD <sup>+</sup> 21]
CuckooOnsai	2021	L3	N/A	AES-CTR	Cuckoo Filter	Hash Tree	[SA21]
ELMI	2022	L3	Y	Flat-OCB (OCB)	Flat-OCB and PXOR-MAC	Counter Tree	[MO <sup>+</sup> 22]
CSI-RowHammer	2023	—	N/A	Optional	PMAC	MACs in ECC bits	[JLK <sup>+</sup> 23]

As a starting point for choosing the components used to implement each Protection Level, we first review the state-of-the-art. Table 1 outlines cryptographic memory protection in various *Trusted Execution Environments (TEEs)*. While the TEE list is not exhaustive (a more complete list is given in [SMS<sup>+</sup>22]), the list of primitives and structures is comprehensive, except for some deprecated methods. (These technologies are detailed in Section 4.2 and Section 4.1.)

We obtain the following groups of alternatives:

1. *The AES vs. a lightweight cipher suitable for memory encryption.* We use QARMA-128, cf. Section 4.1.1. QARMA [Ava17] is a *Tweakable Block Cipher (TBC)*: Beside the secret key and a text, a TBC accepts a *third* input known as a *tweak*, which is used together with the key to select the permutation computed by the cipher. Unlike the key, the tweak may be controlled by an adversary. TBCs simplify the design of modes of operation, with an early application to memory encryption [HT13].
2. *Direct encryption*, where a plaintext block is input to the cipher to compute the corresponding ciphertext, *vs. CounTeR mode (CTR) encryption*, where the encryption of successive counter values results in a *keystream* which is then XOR-ed to the plaintext to obtain the ciphertext (cf. Section 4.1.3 for more details).
3. *Various Message Authentication Code (MAC) algorithms for memory integrity*, such as Carter-Wegman *Universal Hash Functions (UHF)*s [CW79] (for instance, encrypted linear functions of the message), encrypted checksums of the plaintext, or *Parallel MAC (PMAC)* [Rog04] (see Section 4.1.2 for a discussion of the options).
4. *The choice of 32b vs. 64b MACs for the integrity tags.*
5. *Different the sizes of the caches used by the MPE, as well as on-chip memory to store MACs or counters.*
6. *Optionally repurposing some ECC bits to store MACs.*
7. *Different sizes of the memory regions protected by one MAC.* This is obtained both varying the CL size and letting a single MACs cover multiple CLs.
8. *Synchronous vs. asynchronous integrity verification.*
9. *Integrity counter trees with increasing arity.* Their nodes, which in this paper always fit in one CL, contain from 8 to 256 highly compressed counters, one for each child. To achieve this, the operations on the tree guarantee that the most significant bits (for instance 56 bits) of all counters in a node are equal. This common part is stored once in the node, the least significant bits of each counter are stored individually. (See Section 4.2 for more details.) In this paper for the first time we show the advantages of counters split into *three parts*.

We simulate various combinations of the above alternatives in the `gem5` simulator, and run the benchmark suite in these simulated systems with different loads on the memory subsystem. To our knowledge, this is the first evaluation of this type. We also randomize the internal state of the system structures to simulate the more realistic performance characteristics of a not-freshly booted system.

The main two results are the following ones:

- R1** Nearly-transparent strong memory protection is possible with current technology, for client and server systems and in most conditions (cf. Section 5.3 for L1 and L2, and Sections 5.8 and 5.11 for L3. See also Section 6).

**R2** The organization of data structures has the largest influence on system *performance*. Lightweight ciphers clearly outperform the AES in area and power (cf. Section 5.12), but their impact on performance is major only in L1 and L2 schemes (cf. Sections 5.3, 5.7 and 5.8).

More detailed results and observations follow:

- R3** The performance of encryption methods that are based on *direct encryption* methods, such as L1 and L2 schemes, is very sensitive to the latency of the cipher. Moving from the AES to QARMA brings a significant reduction in performance loss. (Cf. Section 5.3.)
- R4** Regarding the previous claim, the performance penalty depends much more on the additional decryption latency on memory reads than on the additional latency induced by encryption on memory writes (cf. Section 5.10).
- R5** Using 32 b MACs in place of 64 b ones halves MAC memory requirements, which is significant. However, MAC memory accesses have poor spatial locality, and the impact on performance is marginal (cf. Section 5.3).
- R6** Small MAC caches have a minor effect on performance. In general, MAC caches are not major performance factors. Counter caches are more effective than the hash caches. The relative improvements due to caching increase with the load of the system. (Cf. Section 5.4.)
- R7** Similarly, using longer CLs (i.e., 128 B instead of 64 B) does not necessarily improve overall performance significantly. However, it halves the memory used by the MACs and enables more aggressive metadata packing in the counter trees. (Cf. Section 5.5.)
- R8** While asynchronous integrity verification improves performance, it is security risk as the system may speculate on potentially corrupted data (cf. Section 5.6).
- R9** If we store *MACs in repurposed ECC bits* (short: MirE) the performance of L2 and L3 schemes has a major improvement — the same applies if the MACs are stored in an internal memory (cf. Section 5.8).
- R10** Incremental MACs, each covering multiple CLs, have a detrimental effect on performance. The optimization of compressing the plaintext to store MACs, whenever possible, together with the payload [TSB18], which serves to reduce the number of memory accesses, cannot be used: Compressibility is a side-channel revealing properties of the data, defeating the purpose of confidentiality protection [Kel02, SBS<sup>+</sup>21]. (Cf. Section 5.9.)
- R11** Increasingly higher arity counter trees offer major and progressive reduction in both memory overhead and performance penalties, despite the complexity of their structure and implementation. (See Table 2 for the memory overheads.) However, as the arity of such integrity trees increases, with the counter group size staying constant, the system must re-encrypt memory or regenerate integrity nodes increasingly often. The use of 3-way split counters substantially reduces the cost of these *Read-Modify-Writes (RMWs)* operations. (Cf. Sections 5.3, 5.8 and 5.11.)
- R12** The most striking finding is that the smaller trees, in fact just their leaf level, are compact enough to be stored in a physically secure, on-chip or in-package memory, that is relatively small with respect to the total RAM, i.e., 1:128 or 1:256. This enables L3 schemes with very low performance penalties. Combined with MirE, they lead to a performance hit of just 3.32% even under extreme bus contention. (Cf. Sections 5.7, 5.8, 5.10 and 5.11.)

## 3 Background

### 3.1 Definitions

Following the Arm terminology [MPS<sup>+</sup>21], a *Realm* is a process domain that is isolated from other process domains through policies enforced by a small TCB. This term encompasses both small *Enclaves* as well as larger *Virtual Machines*.

The SW-accessible volatile, external memory, connected to a memory controller, is seen as an array of blocks. These blocks match the *Last Level Cache's Cache Line (CL)* size and are thus also called CLs.

An encryption or authentication function is said to provide *spatial uniqueness* if, when computed on equal inputs, but written to different locations, it results in different outputs. This is achieved by including the *Physical Address (PA)* of the encrypted or authenticated CL in the computation.

An encryption or authentication function provides *temporal uniqueness (freshness)* when repeated writes of the same plaintext to the same location result in different outputs. This is achieved by including a counter in its computation.

In what follows a mode (of operation) is a general purpose encryption mode of operation. A Memory Encryption (ME) mode is understood to be an encryption mode of operation with plaintext and ciphertext having the size as a CL, and no associated data.

An *on-chip* component is defined as a physically secure block in the same package as the processing elements. In this case the package shall be *tamper-averting*, i.e., a package that is either tamper-proof/resistant, or tamper-evident/detecting.

### 3.2 Adversaries

To adequately answer the question posed in the Introduction, we categorize technologies based on the adversaries they defend against. The adversaries are distinguished according to their access to the target, and their resourcefulness. Before doing this, however, we must make a few critical remarks. Cryptographic memory protection cannot address most side channels, including those that exploit physical effects: These are thus out of scope. The exclusion applies to the access-pattern side channel as well: Adversaries can reverse engineer software properties or elicit secrets from access patterns. The only generic and provably effective mitigation would be *Oblivious RAMs (ORAM)* [Gol87], which carry prohibitive performance penalties. The same applies to SW exploitation, timing attacks and micro-architectural side-channels. For all these threats, mitigations should be applied to SW as needed.

User-space services can always deny resources to Realms, including scheduled time, hence Denial-of-Service attacks must be accepted.

We can now define the following Adversaries:

- $\mathcal{A}^{\text{SW}}$  can run SW on the target, and provide inputs to it, including through external interfaces.
- $\mathcal{A}_{\text{passive}}^{\text{HW}}$  has physical access to the system that contains the target, including its internals, but does not have the capabilities to access on-chip communication interfaces. They can interpose chips and modules for the sole purpose of monitoring transactions.
- $\mathcal{A}_{\text{active}}^{\text{HW}}$ , also performs *active* attacks, e.g., blocking, corrupting, replaying or injecting transactions on the memory bus [KLR<sup>+</sup>20] or other interfaces.
- $\mathcal{A}_{\text{invasive}}^{\text{HW}}$  can mount highly invasive attacks at the chip or package level. Examples range from micro-probing attacks [Sko17] to actual chip reverse engineering and

editing using a Focused Ion Beam Microscope [TJ09].  $\mathcal{A}_{\text{invasive}}^{\text{HW}}$  is out of scope in this paper as the proper defenses require HW countermeasures.

SW and HW-capable adversaries are independent. The HW adversaries form a hierarchy  $\mathcal{A}_{\text{passive}}^{\text{HW}} \subsetneq \mathcal{A}_{\text{active}}^{\text{HW}} \subsetneq \mathcal{A}_{\text{invasive}}^{\text{HW}}$ .

### 3.3 Protection Levels

We provide detailed definitions of the Protection Levels. Table 1 shows how some documented solutions map to them. The technologies used to implement each level are listed. They are taken from options described in Section 2, Table 1. For more details about these technologies, cf. Section 4.1.

#### 3.3.1 L0: Access control

Access control policies to implement *reverse sandboxing* are the first line of defense against  $\mathcal{A}^{\text{SW}}$ . However, RowHammer attacks (and micro-architectural side channels) have significantly increased the power of  $\mathcal{A}^{\text{SW}}$ , enabling them to bypass reverse sandboxing.

Physically separating memory rows of different process domains through access control and precise memory allocation policies could theoretically prevent RowHammer attacks. However, this approach requires complex system software changes and is impractical in real-world scenarios.

We do not discuss the implementation of L0.

*From here on, we assume that appropriate access control policies are in place to stop unauthorized agents within the SoC, but not to prevent RowHammer attacks.*

#### 3.3.2 L1: Memory encryption

*This level provides spatial uniqueness, but not temporal uniqueness.*

Interest in L1 is driven by confidentiality requirements and to make attacks that depend on memory corruption (for instance RowHammer) more difficult. For this reason, L1 must use direct encryption with a cipher that enjoys a strong diffusion property, i.e., any input change induces a flip of each output bit with likelihood 1/2.

In general, protection against  $\mathcal{A}^{\text{SW}}$  is very limited, as is against  $\mathcal{A}_{\text{passive}}^{\text{HW}}$  since the latter can detect ciphertext repeats. Also, note that attacks on the integrity of a system may still cause SW to reveal its contents, therefore this scheme alone does not guarantee confidentiality. Only full replay protection (L3) thwarts the particular attack just mentioned. Warm-boot and cold-boot attacks [HSH<sup>+</sup>09] are properly mitigated. Note that the same arguments apply also to L2.

A common requirement for L1 (and L2) system is the *cryptographic separation* of Realms, which serves to thwart combined SW/HW attacks based on the replay of memory from a target Realm into an adversary-controlled one. This can be achieved by per-Realm unique encryption *differentiators*. (Replay attacks into the *same* Realm, to reset it to a previously known state, require L3 protection.) The differentiators can be encryption keys or, if a single global encryption key is used, bit-strings to be used in a designated bit-field of the tweaks. Differentiators must be discarded upon Realm termination. They should not repeat. If they are tweak contributions, they can be implemented by, say, a TCB-managed 64-bit counter.

*Address scrambling* (a very lightweight encryption mechanism of the PA to permute the memory layout) may also be somewhat effective against RowHammer. It is deployed in some devices like smart cards for the purpose of mitigating side channel attacks. Note that since these schemes are usually static per boot session, address reuse can be detected: this is often all an adversary needs to mount an attack. Hence, it should be considered only as an additional *defense-in-depth* measure and not as a complete mitigation per se.

**3.3.2.1 Implementation aspects.** With the AES, a CL is encrypted in *XOR, Encrypt, and XOR (XEX)* mode [Rog04], as in AMD SEV, TDX, and Apple’s Secure Enclave.

The chosen low-latency block cipher for memory encryption is QARMA-128 (as explained in Section 4.1.1). QARMA-128 is used in a Tweaked *Electronic Codebook (ECB)* mode as in Fig. 2a. In both cases the tweak is the address.

### 3.3.3 L2: Encryption and integrity verification

*This level extends L1 with integrity tags, to detect memory corruption. It does not provide any temporal uniqueness, hence it must rely on a direct encryption method. An integrity tag is usually a MAC. Adversaries can still mount replay attacks.*

L2 targets  $\mathcal{A}_{\text{passive}}^{\text{HW}}$ . It is also partly effective against  $\mathcal{A}_{\text{active}}^{\text{HW}}$ , if they only corrupt individual memory locations or have a limited time budget. To defeat targeted replay of the memory together with the integrity tags, more countermeasures are required (see Level L3 below).

This distinction within  $\mathcal{A}_{\text{active}}^{\text{HW}}$ , though seemingly arbitrary, is necessary due to varying complexities and costs not only of the attacks but also of the *countermeasures*. System designers can assess threats and make business decisions about accepting specific risks. Similarly, active Adversaries might opt for keeping their attacks passive at least initially, to avoid detection and to collect data for cryptanalysis.

**3.3.3.1 MirE: MACs in repurposed ECC bits** If ECC memory is available, storing the MACs in (part of) the ECC bits eliminates the need to reserve normal memory for the MACs, and significantly reduces memory traffic. Note that MACs are still accessible to a HW capable adversary.

The Intel TDX MKTMEi is such a solution. We found no documentation on error correction in a TDX system, but the 28 b MAC field size suggests that a *Single-Error Correction and Double-Error Detection (SECDED)* (255, 247) Hamming code is used. This code is truncated to (143, 135) to cover 128 bits and 7 bits of the MAC each. The remaining 4 bits of the effective 576 bits in each CL are used for parity. This very same configuration is proposed in [YA18].

MirE raises the question of the performance impact of using ECC memory. Reported penalties are smaller than 0.5% [Bac14]. On servers, ECC bits, if not repurposed, are used for error detection, hence memory access times are not affected. In other cases, ECC memory impact is negligible compared to the baseline, so we do not evaluate it as a separate configuration.

**3.3.3.2 Implementation aspects.** The same encryption techniques are used as for L1. For Intel TDX the MAC is computed using truncated SHA-3, with the latency assumed to be comparable to AES-128. In any other MirE scheme, following [JLK<sup>+</sup>23], the tag is computed using QARMA<sub>5-64- $\sigma_0$</sub> . *Note that not all the ECC bits need to be repurposed for a MAC: these bits may contain both a shorter ECC and a MAC.* If the MACs are not stored in repurposed ECC bits, hashing is done by a *multilinear UHF* [CW79] at 32 or 64 bits. Note that these MACs are actually kept as unencrypted *hashes* while on-chip, which speeds up verification, and we encrypt them block-wise when they are evicted from the hash cache groups. For instance, four 32 b hashes are encrypted as a single 128 b block. This enhances system robustness and security against corruption and replay attacks. In schemes with freshness (i.e., L3), the freshness data of the hashes that are encrypted together must be joined to form the common tweak for the hash block encryption.

*Remark 1.* Beside SECDED codes, there are several memory-specific *Reliability, Availability and Serviceability (RAS)* features, with varying levels of redundancy, starting with

Chipkill [IBM99]. These are capable of handling also multiple errors. MirE can be easily implemented in these systems using suitable codes.

### 3.3.4 L3: Encryption, integrity, and replay protection

With respect to L2, this level fully mitigates also against  $\mathcal{A}_{\text{active}}^{\text{HW}}$ , by providing replay protection: In order to replay a CL together with its counter and MACs the adversary either must successfully perform cryptanalysis or wait for a counter repeat. Note that in some variants, the counters themselves may be hidden to the adversary. More information about these data structures is found in Section 4.2.

In a L3 system, a single system-wide key is sufficient for authentication, since nodes closer to the root need to cover memory across Realms. In any case, this is not a security issue. Encryption differentiators are also not required, but they may be a hard customer requirement. Computing integrity tags on the ciphertext ensures that orphaned memory can still be verified, which is essential for secure erasure.

**3.3.4.1 Implementation aspects.** The same freshness information is included in the encryption and in the tag computation. A *Counter mode (CTR)* encryption mode is used with both AES (following AEGIS, the method by Yan et al., and SGX) and QARMA, except with *Encryption for Large Memory (ELM)*, which uses Flat-OCB. The anti-replay technologies are described in the next subsection.

## 4 Review of the Building Blocks

### 4.1 Cryptographic Primitives

#### 4.1.1 Memory encryption primitives

RAM is commonly encrypted using a block cipher: the long initial latency of stream ciphers makes them unsuitable for the purpose.

For simplicity, we only consider block ciphers with a block size of 128 bits: smaller block sizes are used only for smart cards and small embedded devices, and longer blocks are uncommon. The selected block ciphers are the AES [DR02] and QARMA [Ava17], where the second is chosen as a representative of lightweight ciphers. The latencies of most suitable lightweight ciphers are similar (e.g., PRINCE [BCG<sup>+</sup>12]) or worse (for instance SKINNY [BJK<sup>+</sup>16]). To estimate performance penalties for these ciphers, readers can interpolate between our AES and QARMA results. A revised version of QARMA, QARMAv2 [ABD<sup>+</sup>23], has been introduced. Its latency is nearly equal to QARMA's, so we do not consider it as a separate configuration option.

Beside the AES, we do not consider other non tweakable block ciphers. The reason is that as they would require constructions that lead to increased latency anyway. We also do not consider ciphers with block sizes that make them less suitable for memory encryption: For instance SPEEDY [LMMR21] has a block size of 192 bits, and ASCON [DEMS21] in a tweaked mode such as *Masked Even-Mansour (MEM)* [GJMN16] has a block size of 320 bits. (For completeness' sake, given a public permutation  $\pi : \mathbb{F}_2^n \rightarrow \mathbb{F}_2^n$ , we describe an example of a MEM construction: Given a key  $K$ , a tweak  $T$ , and a plaintext  $P$ , all  $n$  bits long, the ciphertext  $C$  is computed as  $C = M \oplus \pi(P \oplus M)$ , where  $M = K \oplus \pi(T \oplus K)$ .)

#### 4.1.2 Authentication primitives

Standard hash functions such as SHA-2 [NIS12] or SHA-3 [NIS15] can be turned into MACs, but the resulting schemes are very slow and not parallelizable.

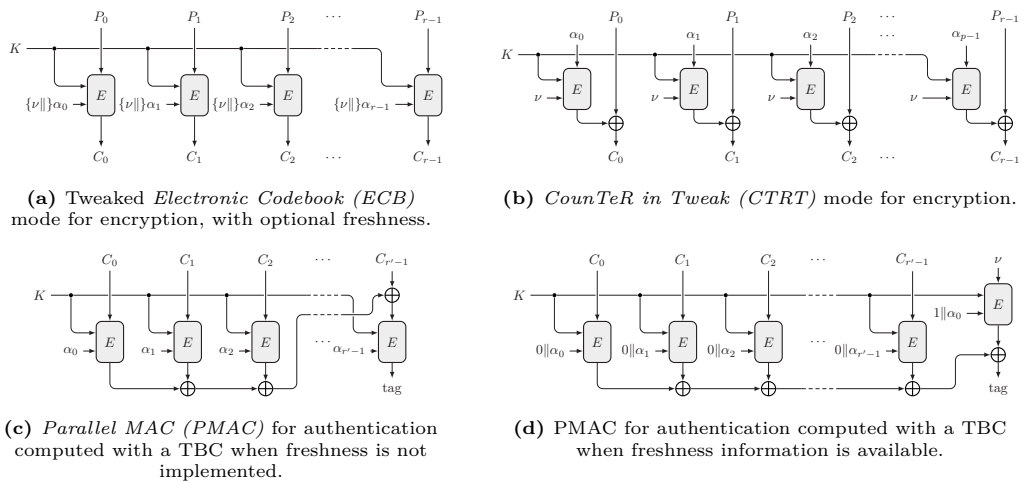


**Figure 2:** Encryption and authentication methods designed around a *Tweakable Block Cipher (TBC)*. They show how freshness can lead to shorter critical paths. Notation:  $E$  is a TBC, the two inputs on the left side of the block being the key (above) and the tweak;  $P = P_0 \parallel \dots \parallel P_{r-1}$ , resp.  $C = C_0 \parallel \dots \parallel C_{r-1}$  is the partition of a plaintext, resp. ciphertext in blocks of equal size;  $\alpha_i$  is the *Physical Address (PA)* of the  $i$ -th block; and  $\nu$  a nonce. If freshness is available, both encryption and authentication algorithms use it, and they share the same nonce. The TBC used for authentication may have a smaller block size than the encryption TBC, in which case  $r \neq r'$ .

Carter-Wegman Hashes [CW79], i.e., encrypted UHFs, are a better choice. UHFs admit fully parallelizable constructions, such as multilinear functions of the input computed over a binary Galois field, as used in SGX [Gue16b]. If there is a MAC cache, it is actually the *not-yet-encrypted* UHF values that are cached, which are thus verified more efficiently.

Apple’s Secure Enclave [App20] uses a *Cipher-based MAC (CMAC)* [IK03] to compute integrity tags. CMAC, being a block-wise chained construction, can not be made parallel and has a high latency, but Apple’s use case does not need very high throughput. It is however unsuitable for general usage requiring high bandwidth and low latency. Instead, we evaluate TBC-based PMACs [Rog04]. PMACs are more expensive than encrypted UHFs, but they can be used for error detection and correction beside integrity, cf. [HS10, SNR<sup>+</sup>18b, JLK<sup>+</sup>23]. The computation of PMACs is depicted in Figs. 2c and 2d. Such constructions can easily be made *incremental* where, upon a write, only the part of the message that has changed needs to be recomputed. A variant for non-TBCs, called PXOR-MAC is described in [IMO<sup>+</sup>22].

Encrypted checksums of the plaintext as in Rogaway’s *Offset Codebook mode (OCB)* mode [Rog04] are an inexpensive method to compute integrity tags, but they suffer from two drawbacks. First, they need to be verified after decryption, potentially worsening overall latency. Second, since they require freshness, a CTR encryption should be used which has lower latency than direct encryption. With CTR encryption, using checksums of the plaintext as the basis for integrity would make the ciphertext malleable, whence a UHF-based MACs should be used instead.

### 4.1.3 Modes of operation

For memory encryption, many (authenticated encryption) modes of operation can be simplified somewhat because the length of the payload is a fixed multiple of the underlying cipher’s block length.

Some older schemes, such as Bastion [CL10], use the block cipher in *Electronic Codebook (ECB)* mode, but the lack of spatial uniqueness keeps plaintext patterns in the ciphertext, therefore modes that provide spatial uniqueness are necessary.

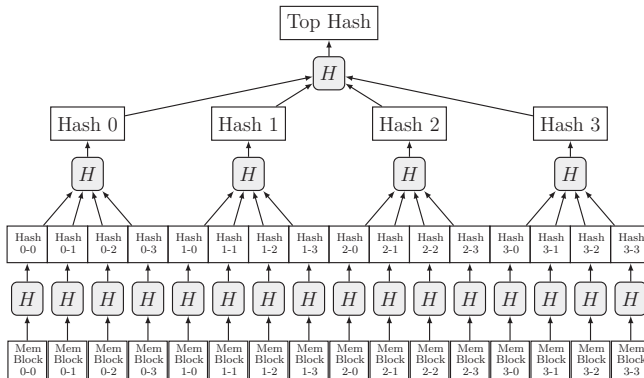


**Figure 3:** Merkle tree.  $H$  is a hash function.

For direct encryption, spatial uniqueness is achieved by using the PA as the tweak. With a non tweakable block ciphers, the latter is used in the *XOR, Encrypt, and XOR (XEX)* construction [Rog04], which is just the XTS mode of operation [IEE19] for a message whose length is a multiple of the block size. XEX is defined as  $C_i = E_K(P_i \oplus M_i) \oplus M_i$ . In other words, a tweak-derived *mask* is added to the input and the output of the cipher. The first mask  $M_0$  is derived by encrypting the tweak, and the successive masks  $M_i$  for  $i \geq 1$  are obtained by multiplying the first mask by a fixed sequence of values. Using a single finite field element  $\gamma$  we can put  $M_i = \gamma^i \cdot M_0$ . Inoue et al. introduce a Flat- $\Theta$ CB mode [IMO<sup>+</sup>22] which is similar to OCB [Rog04]. They define the L3 scheme ELM using Flat- $\Theta$ CB mode for data and PXOR-MAC to authenticate counter groups.

With a TBC, the PA (concatenated with freshness if provided) of each block is used directly as a tweak, cf. Fig. 2a, and a XEX construction is not needed.

In CTR encryption with a TBC, the counter and PA are used as tweak and text respectively (cf. Fig. 2b) to generate the keystream. When not using a TBC, the counter and PA are concatenated and then encrypted.

## 4.2 Memory integrity structures

A table of hashes or MACs protects against memory corruption, but it is not sufficient against replay attacks, unless the table is itself protected. This can be achieved by storing it in a tamper-averting memory or by covering it with a structure such as a *Merkle Tree (MT)* [Mer80] (cf. Fig. 3). MT nodes can be cached [GSC<sup>+</sup>03] to speed up verification.

With freshness-based encryption, we can protect the memory by just protecting the counters, for instance with a *Bonsai Merkle Tree*, i.e., a MT protecting the counter table [RCPS07]. A different method in the *counter tree* (a refactoring of Hall and Jutla’s *Parallelisable Authentication Tree (PAT)* [HJ05]) also used in SGX [Gue16a]. A node of the counter tree is called a *Counter Group (CG)*. A CG contains  $a$  counters, which correspond to the  $a$  children of the node. The counters in a leaf, resp. non-leaf CG are one-to-one with  $a$  CLs, resp. children CGs. A MAC is computed on every node and it is either stored dedicated table, along with the MACs of the data CLs. or in the node’s CL along with the counters. Since the latter approach has better performance, for simplicity we consider only it. The MAC of a CG is computed on the  $a$  counters in the node and the parent counter. Before a node is evicted, its parent counter is first incremented and the node’s MAC is recomputed.

The *split counters* optimization [YEP<sup>+</sup>06] replaces a group of  $a$  counters with a group consisting of a single *major counter* and  $a' > a$  smaller, *minor counters*, associated with that major counter (cf. Fig. 5). A *logical counter* in this scheme is defined as the concatenation of a minor counter and its associated major counter. Each node (a data CL

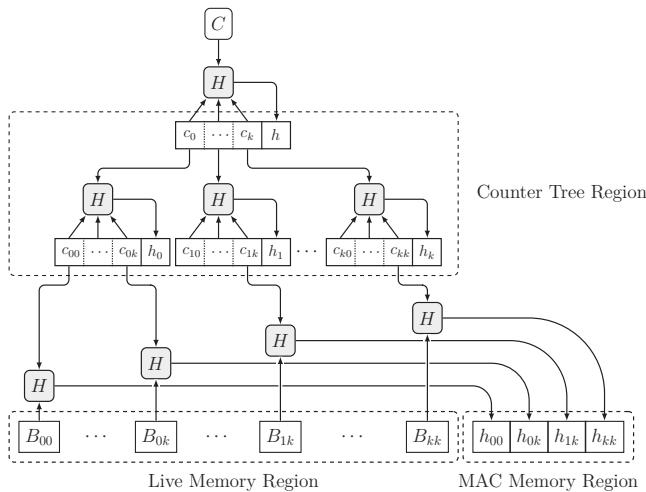


**Figure 4:** Counter tree for memory integrity.

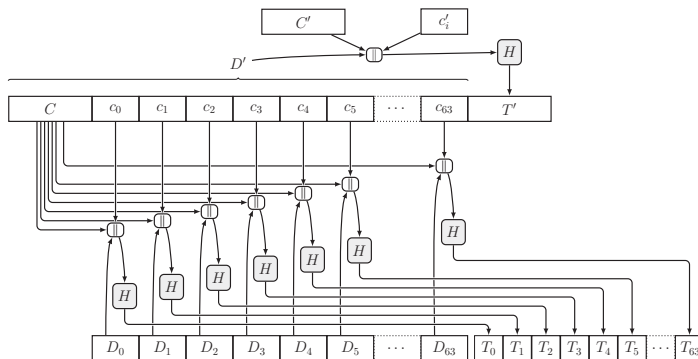


**Figure 5:** Split counters. The  $i^{\text{th}}$  logical counter is the concatenation of a major counter  $C$  (resp.  $C'$ ) and of the the  $i^{\text{th}}$  minor counter  $c_i$  (resp.  $c'_i$ ). This is then used in the function to compute the hash of the  $i^{\text{th}}$  data block (resp. counter group).

or a CG) is associated with a logical counter. The increased arity (for instance, from  $a = 8$  to  $a' = 64$ ) reduces both storage overhead for counters and tree depth. When a minor counter overflows, the common major counter is ticked to ensure that values do not repeat. Since this changes the values of all the logical counters associated with that major counter, all the sibling nodes need to be refreshed. For data CLs this means that they are re-encrypted, and for both types of nodes the MACs need to be recomputed. All minor counters in the group are reset to zero at this point to reduce the frequency of minor counter overflows.

Despite these RMWs, split counter trees bring a major performance improvement over monolithic counters. We introduce here 3-way split counters (with major, middle, and minor counters) to both increase arity *and* reduce RMWs.

Instead of using full trees, two optimizations can be done.

**LoC** One option is storing the data cache line counters in an in-package tamper-averting DRAM (an SRAM would be too large) which is MPE private (i.e., invisible to the rest of the system and outside adversarial control). We call this solution LoC which stands for *Leaves-on-Chip*. In fact, if we store the leaf nodes in a physically protected memory, such as on-chip, then we do not need to compute any other nodes from the original tree. LoC is sometimes mentioned in the literature only to be dismissed as

**Table 2:** Memory Overhead of Various Types of Integrity Trees.

**Legend:**  $\ell_H$ ,  $\ell_c$ , and  $\ell'_c$  are the bit lengths of a hash or MAC; of a monolithic or major counter; and a minor counter, respectively.  $a$  is a counter group’s arity, and  $n$  is the number of CLs a MAC covers.

Type of Tree	CL Length	
	64 B	128 B
Merkle Tree with $a = 4$ , resp. 8	33.3%	16.7%
<i>Monolithic Counter Tree with embedded MAC, <math>\ell_c = 56</math></i>		
• $\ell_H = 64; n = 1; a = 8$ , resp. 16	26.8%	12.9%
• $\ell_H = 32; n = 1; a = 8$ , resp. 16	20.5%	9.79%
• $\ell_H = 32; n = 2; a = 8$ , resp. 16	17.4%	8.23%
• $\ell_H = 32; n = 4; a = 8$ , resp. 16	15.8%	7.45%
<i>Split Counter Tree with embedded MAC, <math>\ell_c = 64</math></i>		
• $\ell_H = 64; n = 1; \ell'_c = 6$ , resp. 7	14.1%	7.04%
• $\ell_H = 32; n = 1; \ell'_c = 6$ , resp. 7	7.84%	3.91%
• $\ell_H = 32; n = 2; \ell'_c = 6$ , resp. 7	4.71%	2.34%
• $\ell_H = 32; n = 4; \ell'_c = 6$ , resp. 7	3.15%	1.57%
• $\ell_H = 32; n = 1; \ell'_c = 3$	7.04%	3.52%
• $\ell_H = 32; n = 2; \ell'_c = 3$	3.91%	1.95%
• $\ell_H = 32; n = 4; \ell'_c = 3$	2.35%	1.17%
PAT with $a = 8$ , resp. $a = 16$	28.6%	13.3%
TEC tree with $a = 8$ , resp. $a = 16$	42.9%	20.0%
128-ary 3-way Split Counter Tree, $\ell_H = 32$	—	3.91%
256-ary 3-way Split Counter Tree, $\ell_H = 32$	—	3.52%
128-ary 3-way Split Counter Tree with MirE, $\ell_H = 32$	—	0.78%
256-ary 3-way Split Counter Tree with MirE, $\ell_H = 32$	—	0.39%

unviable because of the large overhead.

**BoC** A less expensive version of the LoC solution consists of keeping the leaf nodes in external memory and store the level immediately above on chip. We call this tree arrangement **BoC** for *Branches-on-Chip*. Similarly to LoC, the system needs no further levels of the tree to ensure the integrity of the tree. This idea seems new.

#### 4.2.1 Memory overhead comparison

In Table 2, we compare memory overheads of different integrity trees, including the new very high arity trees introduced in this paper. Multi-CL MACs encrypt each CL individually with its own counter, whence the eviction of a CL from the last level cache does not require re-encryption of adjacent CLs. The table also includes the *Tamper-Evident Counter (TEC)* tree [ECL<sup>+</sup>07], which has high memory overhead and requires wide encryption with substantial latency, making it impractical for deployment.

#### 4.2.2 Excluded Methods

*Log Hashes* [SCG<sup>+</sup>03b] are an interesting option because they do not employ a tree structure and have a negligible memory overhead. Log Hashes maintain an incremental hash of a Realm’s entire memory by adding the hashes of all cache lines in it. The hash of a cache line is computed on the concatenation of the contents of the line, its address, and a secret key. The Log Hash is updated with each memory write, by subtracting the contribution of the old contents, and adding that of new contents. Verification of the memory occurs only when the Realm interacts externally. Log Hashes are well-suited only for long-running tasks with minimal I/O, where their performance impact can be negligible. They are unsuitable for general applications and remain unimplemented in practice.

We do not evaluate the *Isolated Tree with Embedded Shared Parity* (ITESP) [TBC<sup>+</sup>20] separately. One of its configurations packs 32 counters in a 64 B cache line where the size of minor counters is 4b, and the freed 128 bits are used to store two 64 b parity/integrity fields, each covering 16 cache lines. We speculate that its performance for a single Realm should be just slightly worse than a 64-ary 64 B split counter groups L3 scheme with MirE, since no MAC table is kept. The closest benchmark that we perform is L3 with 128-ary 128 B split counter groups with 3b minors and MirE. The main benefits of ITESP emerge when multiple Realms run concurrently, a configuration not supported by our setup, because each Realm would have its own integrity tree and metadata cache.

The *CuckoOnsai* (sic) scheme in [SA21] is a quite interesting design. It exploits data compression as [TSB18] to fit a 16-bit counter in a 512 b CL if the contents can fit in 496 bits. We assume that only those 496 bits are encrypted (AES in CTR mode is mentioned) and then the resulting 512 bits are hashed into keys to be stored in an on-chip Cuckoo Filter [FAKM14]. If the CL is not sufficiently compressible, then its counter is protected by a Merkle Tree. Not enough details are provided in the paper to reconstruct the design and in light of the small size of the in-chip Cuckoo Filter it is also not clear how much memory is protected. Since the Cuckoo Filter parameters are missing, the false positive rate cannot be evaluated. In any case, the fact that the counters are just 16 bits long makes the particular design insecure besides the fact that it is also present a data compressibility side channel. Similarly, [NHSQ12], based on Bloom Filters [Blo70], has incomplete description and analysis of the security, while offering only a minor performance advantage with respect to Bonsai MT — which are themselves inferior to proper *Counter Trees (CTs)*. Adding this design them would be inferior to [SA21] because for the same coverage and false positive rate, Cuckoo Filters are more space efficient. We feel that this area of research deserves more attention, but the current literature has not yet reached a sufficient level of maturity and the schemes proposed so far fail basic security scrutiny. Therefore, we do not evaluate these schemes in our study.

### 4.3 Cryptographic parameters and practices

To ensure long-term confidentiality, *encryption keys should be at least 128 b long*. Shorter keys are not used in any currently deployed or recently proposed memory protection scheme. Sometimes longer keys are an option, for instance 256 b keys for Intel’s TDX, but we posit that this does not offer increased practical security and only increases latency: indeed, a proper complexity analysis of quantum-computer-assisted key search against AES-128 proves it is secure even against adversaries with access to a large-scale quantum computer [JNRV20]. Deployed technologies such as Intel’s SGX and TDX, and AMD’s SEV use the AES in modes that need two independent keys, or even AES-256. QARMA-128 and QARMAv2-128 allow the use of 256-bit keys as well.

*Encryption block sizes must be at least 128 b*, to reduce the likelihood of any attack that exploits ciphertext collisions.

*Authentication keys should be at least 128 b long as well.*

Only the TCB and no SW environment may set any key, and SW will only manage process identities.

*We posit that a length of 32 b (or even 28 b) is sufficient for both data and counter group MACs, to deter Adversaries that simply want to corrupt memory, for instance with RowHammer attacks.* This is, in fact, one of the main reasons to deploy a L2 scheme. The TCB must destroy (i.e., internally invalidate and overwrite) the key or tweak associated with the address where an integrity violation occurred — and possibly other internal information. The target process will no longer be able to execute, and the information in it will be lost to the adversaries. It is essential that the TCB responds so to integrity

violations before giving back control to the operating system or the hypervisor. Otherwise, to make just one example, an  $\mathcal{A}_{\text{active}}^{\text{HW}}$  adversary with the ability to run privileged SW would be able to brute force a short MACs.

If the chosen authentication primitive produces a longer MAC than needed, the output is simply truncated.

In L3 schemes, an Adversary may attempt to replace a CL together with its MAC. To do this without triggering an integrity fault, they wait until the counter associated with the target CL repeats. If the counters are sufficiently long, the attack cannot succeed. For this reason, monolithic counters must be at least 64 b long (it can be argued that 56 bits suffice). The minimal aggregated length of a major and a minor counter (or major plus middle plus minor) shall also be 64 b. If an Adversary wants to replay a CL together with its MAC and counter, they will similarly have to either guess the embedded MAC or wait that the parent counter repeats.

For Merkle Trees the minimal hash length is 128 b, to ensure that attacks have a time complexity of at least  $2^{64}$ .

## 4.4 On the design space

In Fig. 1 an MPE is associated with a memory channel, benefitting from memory interleaving and thus reducing bandwidth saturation risks. In the figure an MPE is also represented as a separate block between system cache and memory controller, but this is far from the only option: it can be implemented as part of the memory controller or a wrapper around the system cache. A different MPE configuration involves a core-private MPE, positioned upstream of the on-chip interconnect. In such a design, the MPE can be a performance bottleneck, but it is suitable for *secure cores*, like SoC-embedded TPMs.

Pure SW solutions are possible: At boot, a part of a cache is *address locked* in order to keep the TCB in it (and effectively reducing its size). All memory reads/writes to external memory are then trapped to this code to augment them with encryption and integrity support. Performance is clearly severely impacted, as in [CZG<sup>+</sup>15, MMS<sup>+</sup>20]. A different, less secure, approach [Pet10, GMD<sup>+</sup>16] keeps most of the RAM encrypted except for a few recently used pages, which are re-encrypted once they have been idle for some time.

Recall that we only consider solutions contained in the SoC package. This excludes any form of “smart memory” [AN17] where the protection logic is split between the Requester and the Completer, such as the *CXL.memory Integrity and Data Encryption (IDE)* scheme [CXL19]. Such architectures require logic for attestation, secure link setup, and encryption, involving cryptographic engines in every memory module if not every chip, so it would be more expensive, hardware-wise, than an MPE-based solution. CXL is however suitable for disaggregated memory configurations, covering transport between compute and memory nodes.

*The breadth of the subject and constant developments (cf. Table 1) imply that the full design space is likely not knowable. The present work represents just a snapshot.*

# 5 Benchmarking plan, results, and discussion

## 5.1 Benchmarking environment and methodology

It would be impractical to implement several thousands of combinations of technologies in silicon for the purpose of evaluating them. A solution to this problem lies in prototyping, i.e., the creation of an approximate implementation of the desired features, which can thus be tested and benchmarked. Very accurate models can be created even without implementing all details. For instance, the latencies of cryptographic primitives can be derived from actual implementations and inserted as delays into the simulation.

The prototypes used in this paper are built in the `gem5` simulator [BBB<sup>+</sup>11,LAA<sup>+</sup>20]. `gem5` allows engineers to build SW versions of HW components typically included in computer systems. It abstracts the interfaces between components, which can be combined flexibly. It provides approximate timing models for many processor cores.

The modeled CPU core is an Arm Cortex A72 with a 2 GHz frequency and a 1 GHz system frequency. The cache hierarchy includes L1-I (48 KiB, LRU replacement policy, 3-way set associative, 1 cycle latency) and L1-D (32 KiB, LRU replacement policy, 2-way, 1 cycle latency) caches, and a unified L2 cache (1MiB, tree-PLRU replacement policy, 16-way, 5 cycles latency). The memory is 16 GiB DRAM in a dual-rank DDR4 DIMMs. The MPE-private caches are 4-way set associative with an LRU replacement policy.

The simulated SoC is implemented in a 7 nm process. We take the latencies of some components from [Ava17], for instance 15.76 ns for a pipelined implementation of AES-128, 4.8 ns for QARMA<sub>11</sub>-128- $\sigma_1$  and 2.2 ns for QARMA<sub>5</sub>-64- $\sigma_0$ . Note that implementation, process, libraries all affect the crypto block’s latency, but system and CPU clocks do not. We assume we reuse the IP blocks from [Ava17] with their own clocks, thus with the exact same performance characteristics. This is a reasonable assumption since this is how hard macros are used in practice. The above latency of QARMA<sub>5</sub>-64- $\sigma_0$  is also used in [JLK<sup>+</sup>23], and essentially for the same purpose as ours.

Lastly, all MPE algorithms are thoroughly parallelized to their maximum extent for all considered schemes.

Our evaluation uses the SPEC 2017 [BLvK18] benchmark suite. Detailed software models such as `gem5` increase execution time by several orders of magnitude: a typical SPEC benchmark can take around a month to run [San14]. To facilitate rapid prototyping, we use the SimPoint [SPHC02] methodology, which is well understood in academia and industry. It uses clustering to find representative regions that serve as a proxy for the whole application. The results are finally combined using weighted averages, that reflect the regions’ importance to the overall application. Up to 10 SimPoints of 30 million instructions from each benchmark are simulated in place of several billions of instructions. (Regarding reproducibility, including all details needed to re-generate our SimPoints would be impractical — for instance, even the choice of compiler affects their offsets.)

An alternative approach would have been to run the entire benchmarks, as opposed to SimPoints, in parallel on a large distributed cloud. This unfortunately does not work in practice since the longest running workloads would have taken weeks to months to run to completion while providing few or no benefits compared to SimPoints. The quicker turnaround, less than an hour to run all SPEC 2017 on a big-enough cluster, is in fact instrumental when exploring a vast space of optimizations. Some papers do this because only very few schemes or benchmarks are run.

A legitimate question is whether we can verify the reliability of our simulations by porting SPEC2017 to run under Client SGX. This would be a major undertaking, even with the help of general-purpose wrappers, we would have to avoid the penalties related to the *Enclave Page Cache (EPC)*. In fact, [Gue16a], only runs `445.gobmk` from SPEC2006 with selected data sets. This said, on the `trevorc.tst` and `nngs.tst` data sets, [Gue16a] reports performance penalties of 4.90% and 3.29%, respectively, and on our simulated SGX-like method we measure 5.31% and 4.65%, which are in line to what one would expect from a deeper tree.

Regardless of how the simulation is performed, we may ask ourselves about the impact on systems that include context switches, virtual memory swap, and any type of I/O. These aspects are very difficult to emulate. In fact, benchmarking in such a context seems absent from the literature on cryptographic memory protection. However, we can observe that (i) The additional memory used for metadata is not visible to the operating system and will be unaffected by paging and similar operations; and (ii) It can be argued that context switches, paging, and general I/O are affected by the performance penalties on

memory accesses only in a minor way: context switch code and data can reside in pinned memory, and the timing of disk, network operations is dominated by media which are orders of magnitude slower than physical RAM. Speaking in particular of context switches, consider a CPU-intensive task running on a 128-core shared machine with about 500 active user sessions. There are 70 unique users on the machine, many of them running a full GNOME environment, with a 15-min average load level of 65 (which is very high). We observe less than a handful of context switches per second per core. Any cold start effect after the context switch would be in the noise since warming all the caches take just a few million instructions (roughly a few milliseconds).

*Therefore, any performance penalty we present here is likely an upper bound to the real-world one.*

## 5.2 Selection of the benchmarking sets

All MPE configurations span a vast multidimensional space. Exhaustively evaluating them all is clearly infeasible, not to speak of the difficulties of properly presenting the data. Hence, we explore the design space in various stages, each consisting of a *set* of runs of the benchmark suite. Each set focuses on some previous configurations and expands the parameter space *where we expect that it has some noticeable impact*. Some schemes, such as L1 schemes, do not carry over to the successive sets because they do not have implementation parameters beyond the encryption primitive.

We use shorthands to describe the various configurations:

Level / Cipher / {additional technologies} / MAC length / CL length .

The optional “additional technologies” may include: counter representation (*mono* or *split*) and arity, Leaves or Branches on Chip (*LoC* or *BoC*), or the use of MACs in Repurposed ECC bits (*MirE*).

The default CL length is 64 B, unless the counter groups are on chip, in which case it is 128 B. The default MAC length is 56–64 b.

“{AMD} SME” is equivalent to L1/AES/GFmul/CL64B. Here, GFmul denotes a XEX scheme where the tweaking mask is computed by multiplication of the tweak by an additional secret key, whereas when we just write XEX the mask is derived by encryption of the tweak; “{Intel} TDX” is equivalent to L2/AES/MirE/28b/CL64B, and “{Intel} SGX” is based on Client SGX, i.e., L3/AES/mono-8/56b/CL64B. LoC always implies counters are split. L2 implies that a non tweakable block ciphers is used in a XEX construction, except when explicitly stated otherwise. The shorthand L3/LoC denotes a version of L3 that uses LoC, and thus no integrity tree. Similarly, L3/BoC is a L3 solution with the leaf counters off chip and the next level on chip, also without a full tree. L3 *without* BoC or LoC denotes a replay-protection-capable scheme based on an integrity tree and *no counters on-chip*.

### 5.2.1 Simulation of system load

The benchmarks are first run on an *unloaded* system, where the current benchmark is the only running task.

We then want an upper bound for the performance degradation in a fully *loaded* system, with up to hundreds of processes running on dozens of processing elements, all sharing the bandwidth of the memory subsystem, such as in a cloud server. Directly simulating such a system is very complex and impractical. We instead inject synthetic traffic upstream of the MPE, but after the L2 cache. We do not include a L3 cache in the system to simulate the extreme situation where the latter has been completely swamped by traffic coming from other requesters or clusters of requesters.

The question is then, how much extra traffic we must inject.

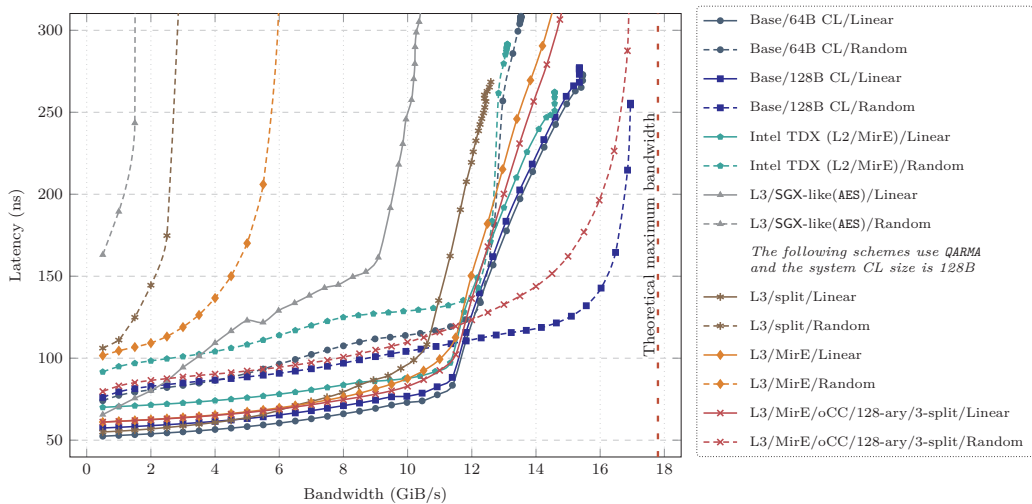


**Figure 6:** Bandwidth/latency plot with various MPEs and without, for linear or random synthetic traffic.

Therefore, we measure the effective memory latency of the system with various levels and schemes of memory protection, and we observe that the latency starts to degenerate catastrophically for most of them between 8 and 10 GiB/s. Fig. 6 shows how latency, and thus, at least part, also performance penalty depend on the load of the system. For instance, a SGX-like L3 MPE covering the entire memory starts to degrade if more than 8 GiB/s of traffic is injected. We take this value as the traffic for a fully-loaded system and halve it, i.e., 4 GiB/s for the partially-loaded system.

The simulated traffic consists of 75% reads and 25% writes of entire cache lines (64 B or 128 B). The access pattern is a mix of cache-line-aligned linear and random accesses. The linear accesses are sequential, and the random ones are at randomly generated addresses, both across the whole reserved range. The traffic generator alternates 100  $\mu$ s of simulated time of linear accesses with 200  $\mu$ s of random accesses, for as long as the workload is running.

Beyond 8 GiB/s (actually, beyond 8 GiB/s *per rmemory channel*), we expect a cloud provider to counter performance deterioration by migrating VMs to other machines to balance load and meet overall performance targets. This would also bring MPE penalties back under control.

### 5.2.2 Baseline performance

Without memory protection, our benchmarks run on a loaded system 14.1% slower than on an unloaded system with 64 B CLs, and 9.5% slower with resp. 128 B CLs. Changing the CL length from 64 B to 128 B results in an average speedup of 1.4% in an unloaded system and 5.5% in a loaded system.

The timings of all benchmark runs are always compared to the baseline with the same load and CL size.

### 5.2.3 Initialization of short counters

When a piece of software starts to run, in a real-world setting any minor/middle counter will have assumed, because of previous processes, essentially random values. If all counters are initialized to zero before running a benchmark, the latter is put at an advantage, since the non-major counters will take longer to overflow, and the number of RMWs may be

underestimated. In fact, the use of SimPoints may even amplify this bias. Therefore, to make our simulations as realistic as possible, in all split counter runs we initialize the non-major counters to uniformly random values. This magnifies the performance gap between 2-way and 3-way split counters of equal arity, highlighting the superiority of the latter.

*We now report and discuss the results of all the runs.*

### 5.3 Set 1: State-of-the-Art, AES vs. Lightweight encryption ciphers, and 64 b vs. 32 b MACs

*We start with the state-of-the-art and some simple variations thereof to get an initial overview of the relative performance merits of the deployed or proposed technologies. We compare L1/AES/CL64B (e.g., AMD SME), L1/QARMA/CL64B, L2/AES/32b/CL64B, L2/AES/MirE/28b/CL64B (corresponding to the Intel TDX and Scalable SGX MKTMEi), L2/QARMA/32b/CL64B, L2/QARMA/MirE/32b/CL64B, and ELM with both monolithic and split counters, SGX (i.e., memory protection as in Client SGX, but covering all memory, L3/QARMA/split-64/32b/CL64B — all with and without a hash cache if not fixed by the manufacturer’s architecture, since some architectures have a hash/MAC cache while other ones, such as SGX, avoid it. We also compare 32 b and 64 b MACs in selected cases — shortened to 28 b, resp. 56 b, in TDX, resp. SGX.*

Note that SGX here is not a full implementation of Intel’s Client SGX architecture, but only of its encryption, integrity, and anti-replay features, the latter expanded to the whole memory. For SGX, hash encryption is CTR as described by Intel [Gue16a]. We use this method for the SGX-like variant with AES-256 (L3/AES256/mono-8/56b/CL64B) as well. In all other cases, data MACs are replaced by 32 b long hashes which are directly encrypted in groups of four upon eviction.

Note that TDX includes also Scalable SGX.

The ELM method follows [IMO<sup>+</sup>22], i.e. it uses the AES in a XEX construction except when QARMA is used. With QARMA the XEX constructions are replaced by simply feeding nonces and separation fields as the tweak to QARMA, as well as using QARMA<sub>5</sub>-64- $\sigma_0$  to generate the *One-Time Pads (OTPs)* to encrypt the tags.

Note that monolithic counter trees are 8-ary, resp. 16-ary with 64 B, resp. 128 B CLs. For 2-way split counters, minor counters are always 6, resp. 7 bits long, and the arity is therefore 64, resp. 128.

For schemes that provide freshness, the counter cache is 64 KiB as in SGX to level the comparisons.

These principles apply to every successive set as well, except where explicitly indicated otherwise.

The runs reported in Fig. 7 support Results **R2** and **R5**. Also, ELM has worse performance than SGX, having the encryption primitive on the critical path.

Recall that the latencies of AES-256, AES-128, and QARMA-128 in our simulation are 21.99 ns, 15.67 ns and 4.80 ns, respectively. They are strongly correlated to the corresponding performance penalties of a L1 scheme on an unloaded system: 7.93%, 6.37%, and 3.21%. Similar outcomes hold also for varying loads and L2/MirE schemes. For L2/non-MirE and L3 schemes, the difference becomes less significant as the slowdown due to traffic contention between data and metadata increases. This proves Results **R3**.

*For the remainder of the evaluation, because of Result **R5**, for simplicity’s sake we shall assume that MACs are 32 bits long and directly encrypted in groups of four except with SGX, MirE, or otherwise explicitly indicated. Similarly, since split counters perform better than monolithic counters (this goes towards Result **R11**), we shall assume that L3 configurations will make use of split counters.*

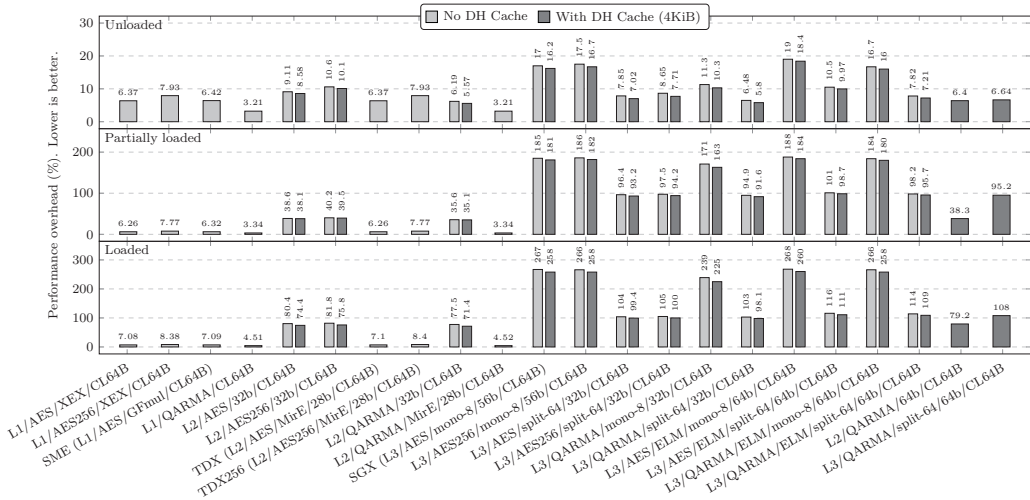


**Figure 7: Set 1** (Section 5.3). Comparison of base levels and state-of-the-art.

For brevity, in Sets 2, 3 and 4 we leave out AES from the comparison as it has an identical memory access pattern and similar results to using QARMA-128.

## 5.4 Set 2: Impact of MPE cache sizes

The goal here is to understand the impact of the sizes of the two MPE caches, namely the hash and counter caches.

L1 does not need caches, so we only consider L2 and L3.

The hash cache sizes we evaluate are 4 KiB, 16 KiB, and 64 KiB; and counter cache sizes are 16 KiB, 64 KiB, 256 KiB, and 1 MiB. We expect these sizes to be within a reasonable range when implemented as SRAM. The presented results are based on the L2/QARMA/32b/CL64B and L3/QARMA/split-64/32b/CL64B configurations (i.e., 32 b MACs, 64 B cache lines, and 64-ary split counters for L3).

These results, displayed in Fig. 8 support Result **R6**. The small benefit of the hash cache can mostly be attributed to spatial locality (most temporal locality has already been exploited by normal data caches). Intuitively, the access patterns of the counter and the hash cache should be similar. However, the reach of the counter cache is bigger since counters are smaller when using split counters and nodes closer to the root cover a large amount of address space which makes them more likely to be reused.

Starting with Set 3, the MPE has a 16KiB hash cache and a 256KiB counter cache. Level L3 uses split counters, unless explicitly indicated otherwise, or with SGX.

## 5.5 Set 3: Impact of the cache line length

Another fundamental piece of information is how the choices of 64 B and 128 B CLs affects L2 and L3 performance: Doubling the CL size will halve the memory overheads, but at least in theory the coarser memory granularity may negatively affect performance.

This set comprises L2/QARMA/32b and L3/QARMA/split/32b with 64 B and 128 B cache lines. Counter group and CL sizes are always equal which implies that L3 split counter configurations have arity 64 in the 64 B case and 128 in the 128 B case.

The results of Set 3 are combined with those of Set 4 in Fig. 9. They prove Result **R7**. Since we already know that our reference system without an MPE performs 1.4% to

5.5% better with 128 B CLs, we expect that using to 128 B CLs, at least for the system cache, is generally beneficial in a system with an MPE.

We acknowledge that changing the cache line size for the coherent cache system might be a major undertaking. However, there are important cases where it is feasible and reasonably non-intrusive. For example, inclusive last-level caches (LLCs) could store and perform writebacks of pairs of 64 B cache lines while still performing coherence on the individual lines. Similarly, LLCs outside the coherent domain (system caches) may use 128 B cache lines while the coherent caches use 64 B cache lines. Both options make the effective cache line size 128 B from the point of the MPE.

## 5.6 Set 4: Asynchronous MAC verification

*So far, we have assumed that integrity tags are verified synchronously. In principle, asynchronous verification can improve performance by releasing data to the CPU before its MACs has been fetched from memory and verified. Therefore, we assess how synchronous verification improves overall performance over asynchronous verification.*

We test only L2 and L3, as they offer integrity. We reuse the configurations of Set 3. The results are shown in Fig. 9.

Asynchronous verification comes with a significant drawback. Since the CPU is speculating on MAC verification being successful, adversaries have a window of opportunity where the CPU is using data under their control and mount an attack. Mitigating this issue introduces significant complexity which would be detrimental the integrity of the system. This is Result R8.

*From here, we only use synchronous MAC verification.*

## 5.7 Set 5: Use of on-chip memory for L2 and L3

*Going beyond caching as explored in Set 2, we explore the impact of secure MPE-private on-chip memory.*

Since MACs have a larger memory overhead than counters, we do not expect schemes with on-chip hashes and off-chip counters. Hence, we ignore such a configuration.

Fig. 11 results confirm that relieving the memory bus contention between data and metadata improves performance.

The BoC configuration only marginally outperforms the schemes that do not rely on on-chip memory. This is explained by considering a system without on-chip memory: Temporal locality is poor for leaf nodes, but it improves closer to the root of the tree as each node corresponds to a large memory space. This makes it likely that integrity verification encounters a cache hit at the level just below the leaf level. Therefore, performance is similar to BoC .

With all metadata on chip, the performance is close to the baseline. This may not be realizable in practice. However, as we shall see in Section 5.8, it can be approximated by repurposing ECC bits for MAC storage.

For this set of runs we kept the AES to show that for L3 the performance is similar to QARMA. However, on an unloaded system, AES and QARMA show a slight performance gap. This gap decreases as the system load increases, due to the fact the cipher latency becomes proportionally smaller compared to the increasing memory access latency.

## 5.8 Set 6: Impact of repurposing ECC Bits, 3-way split counters, and large counter caches

*The deployment of Intel TDX's Multi-Key Total Memory Engine with Integrity (MKTMEi) [Int21] and [YA18] suggests that using ECC bits for tags may be an acceptable trade-off*

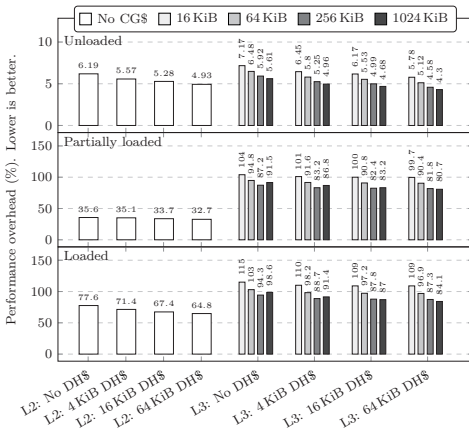


**Figure 8: Set 2** (Section 5.4). Impact of MPE cache sizes on L2/QARMA/32b/CL64B and L3/QARMA/split-64/32b/CL64B.

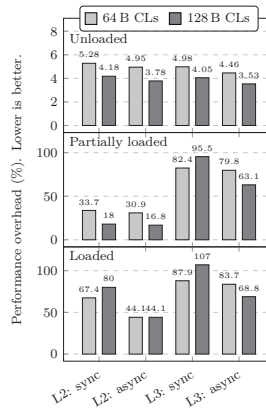


**Figure 9: Sets 3 and 4** (Sections 5.5 and 5.6). Impact of CL size and asynchronous MAC verification.

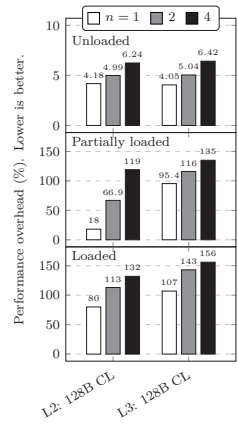


**Figure 10: Set 7** (Section 5.9). Impact of incremental MACs.

for real-world deployments. This is essentially an approximation of storing MACs on-chip since the ECC bits are stored out-of-band and fetched in parallel with the data.

We consider both L2 and L3 configurations, with and without MirE. We expect that MirE implementations are optimized for performance and to reduce storage overhead. For that reason, except for L1/QARMA/MirE/CL64B, we focus on 128 B CLs which enable denser counter packing than 64 B CLs. With MirE the MAC algorithm is PMAC, and a hash cache is not needed since MACs and data are fetched in the same memory transaction.

In addition to classic 2-way Split Counter Groups (CGs), we introduce high-arity 3-way Split CGs, which we define only in the length of 128 B, with 128 and 256 logical counters per node. The purpose of this optimization is to keep the amount of RMW operations under control, with one variant also increasing the density of the CGs. To quantify the impact of this optimization, we evaluate each configuration with and without middle counters. We consider the following 3-way split CG types, without embedded MACs:

- 128 × 7 b minor, 8 × 8 b middle, and 1 × 64 b major counters, with a memory overhead of 1:128; and
- 256 × 3 b minor, 32 × 6 b middle, and 1 × 64 b major counters, with a memory overhead of 1:256.

If MACs are embedded in the counter group, for a 128-ary tree the lengths of the major and middle counters would be reduced to 48 and 6 bits, and for a 256-ary tree the middle counters would be 5 bits long – in both cases with 32 b MACs. The memory overheads of these trees are 1:127 and 1:255.

In [YA18, SNR<sup>+</sup>18a] “delta encoded” split counters with rebasing are used together with methods to accommodate a limited number of larger minor counters in a CG to reduce the amount of RMWs. We skip these optimizations since our 3-way split CGs (cf. also Section 5.11) perform better, by nearly eliminating any RMW overhead.

The data (Fig. 12) supports Results R9 and R11. Middle counters play a crucial role in maximizing the performance of high-arity CGs, preventing significant RMWs overheads. This demonstrates Result R12. Because of this, L3/MirE/LoC designs may even perform better than L1 schemes, which have the cipher on the critical path to the external RAM.

For a 16 GiB protected memory, the BoC configuration needs 256 KiB of on-chip storage. An alternative to the BoC configuration would be to use that memory for a counter

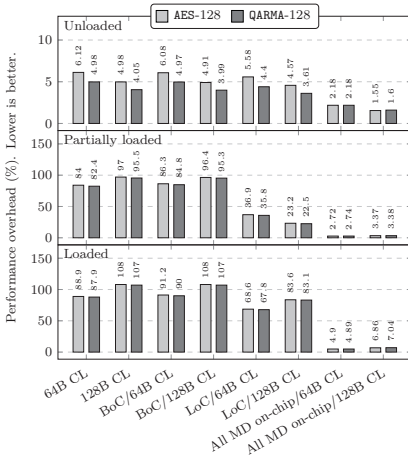


**Figure 11: Set 5** (Section 5.7). L3: Impact of storing metadata on-chip.

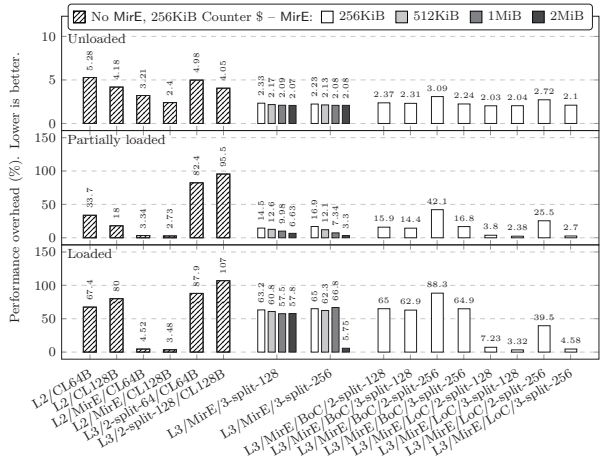


**Figure 12: Set 6** (Section 5.8). {L2/L3}/QARMA/MirE: Impact of repurposing ECC bits for MACs and large counter caches. For arity 128 or 256 the CL is always 128 B.

cache. The 512 KiB configuration in Fig. 12 corresponds to this configuration since the baseline counter cache size is 256 KiB. In such cases, the larger cache normally performs on-par with BoC in an unloaded system and slightly better under load. This can be explained by two effects. First, the cache approximates BoC since the level just above the leaf level is very likely to be resident in the cache. Second, unused branch nodes can be replaced by useful leaf nodes which improves efficiency. On a fully loaded system, LoC performance is reached in practice only when the cache is large enough to cover the tree working set of the running applications. In the case of SPEC 2017, this typically happens between 1 MiB and 2 MiB of cache.

## 5.9 Set 7: Impact of incremental MACs

*If we cannot store MACs in the ECC bits or on-chip, there is another option for reducing their storage overhead: to compute them incrementally over multiple cache lines.*

Since the goal here is to reduce storage overhead, we consider only 128B CLs. We test both L2 and L3 configurations with a MAC covering 1, 2, or 4 CLs. The runs are reported in Fig. 10. We use only QARMA-128 for encryption, since the performance degradation depends only on the increased memory traffic. In fact, AES results follow the same pattern. These measurements prove Result R10.

## 5.10 Set 8: Breakdown of selected configurations

To better understand the behavior of the MPE, we select a few interesting configurations and show all individual benchmarks in the suite:

- AMD SEV (L1/AES/GFmul/CL64B) and L1/QARMA/CL64B;
- Intel TDX (L2/AES/MirE/28b/CL64B);
- L2 with (L2/QARMA/MirE/28b/CL64B) and without (L2/QARMA/64b/CL64B) MirE;
- Intel SGX (L3/AES/mono-8/56b/CL64B);
- 128- and 256-ary 3-way split CGs (L3/QARMA/LoC/3-split-128/MirE/28b/CL128 and L3/QARMA/LoC/3-split-256/MirE/28b/CL128).

The SPEC2017 benchmarks (cf. Figs. 13 to 18) exhibit some expected results: certain tasks, like `omnetpp`, `mcf`, and `bwaves` experience a more significant performance impact across most MPE configurations.

Fig. 13 supports the claim in Result **R4**. The two XEX schemes `L1/AES/GFmul/CL64B` and `L1/AES/XEX/CL64B` differ only in the computation of the tweaking mask. In the first case it is performed via Galois multiplications, which we highly optimize for speed, resulting in a latency of 0.55 ns in the chosen process. In the second case AES encryption is used instead. We recall that AES-128 latency is 15.76 ns. Thus, on the write path, the latency is, roughly one, resp. two AES instances, while on the read path is it always one AES instance. Despite the significant difference on the write path, the penalties are almost exactly the same.

## 5.11 Set 9: Impact of RMW operations

*All split counter methods need, as already mentioned, to perform some batches of RMW operations to re-encrypt data or re-compute some embedded MACs whenever a minor, resp. middle counter overflows. These are expensive operations and we want to understand their impact on performance.*

We compare the performance of L3 MPEs against hypothetical ones where the RMW operations have zero cost, i.e., are instantaneous. This is achieved by simply skipping them: such an experiment is possible because the simulated MPE does not actually perform cryptographic operations, inserting instead timing delays in their places. This gives an upper bound on the actual time spent in the RMW operations.

For the 128- and 256-ary split counter schemes, we report the performance with 3-way split counters, the performance with 2-way split counters by omitting the middle counters, and the performance with skipped RMWs. The selected combinations are the ones in Set 8 with RMWs.

The results are shown in Figs. 17 and 18. We notice that the impact of RMWs is not always negligible. Using 2-way split counters with 3b minors (L3/QARMA/LoC/MirE with 256-ary CGs) carries a significant performance penalty, but the use of middle counters brings the performance close to the ideal case where RMWs are “free”.

The performance penalties and the proportion of time spent doing RMWs increase with the load.

This set of runs proves Results **R1**, **R11**, and **R12**.

## 5.12 Remarks on area and power

Power consumption of a circuit is roughly a linear function of both its area and the time it is active.<sup>1</sup> Thus, the MPE’s total area and the performance penalty are the main factors determining its energy cost.

The area of the MPE mostly consists of arithmetic circuits, caches, and any internal DRAM (if present). In comparison, the control circuitry has negligible area.

Not only is estimating areas for all configurations impractical, but also implementations can vary greatly. For direct encryption schemes like L1 and L2, implementing multiple encryption blocks in parallel maximize performance, but area can be saved by sacrificing some of that performance using pipelined designs. An area-optimized implementation of QARMA-128 (with 256-bit keys) is roughly  $\approx 50$  KGE for a single pipelined block [Ava17]. Latency-optimized AES implementations exceed 17 KGE per round [UHM<sup>+</sup>20], hence the area for a single instance is  $\approx 160$  KGE and for eight parallel blocks  $\approx 1.3$  MGE. Note,

<sup>1</sup>To be more precise, power consumption is the sum of dynamic power, that depends on switching current, and static power, that depends on leakage current, and thus on power gating.

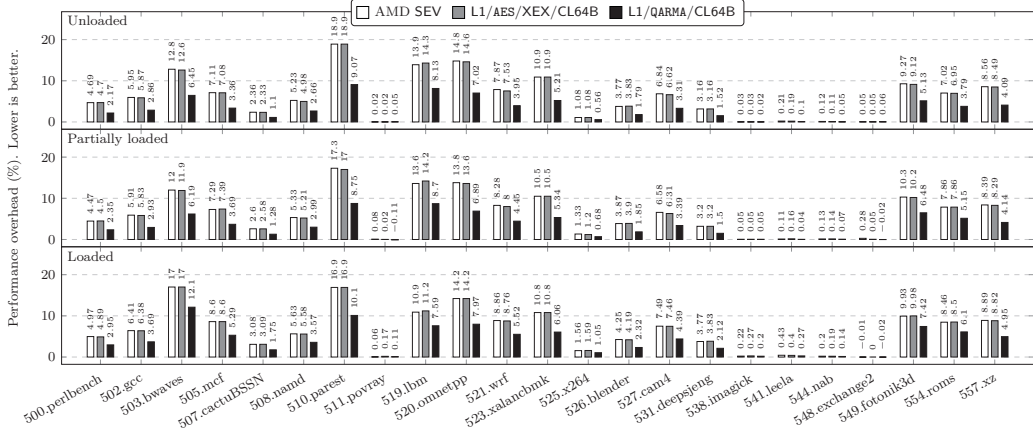


**Figure 13: Set 8** (Section 5.10). Comparison of AMD SEV (L1/AES/GFmul/CL64B), L1/AES/XEX/CL64B, and L1/QARMA/CL64B.

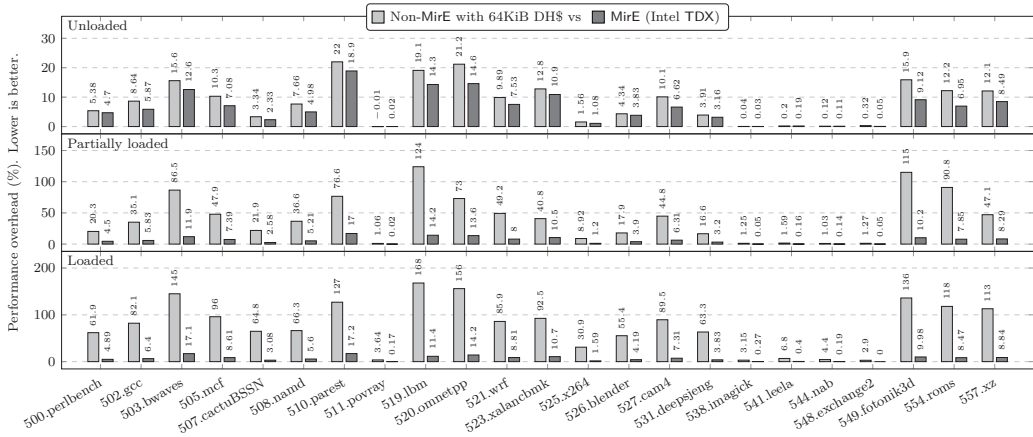


**Figure 14: Set 8** (Section 5.10). L2 impact of MirE: L2/AES/32b/CL64B vs. L2/AES/MirE/28b/CL64B (e.g., Intel TDX).

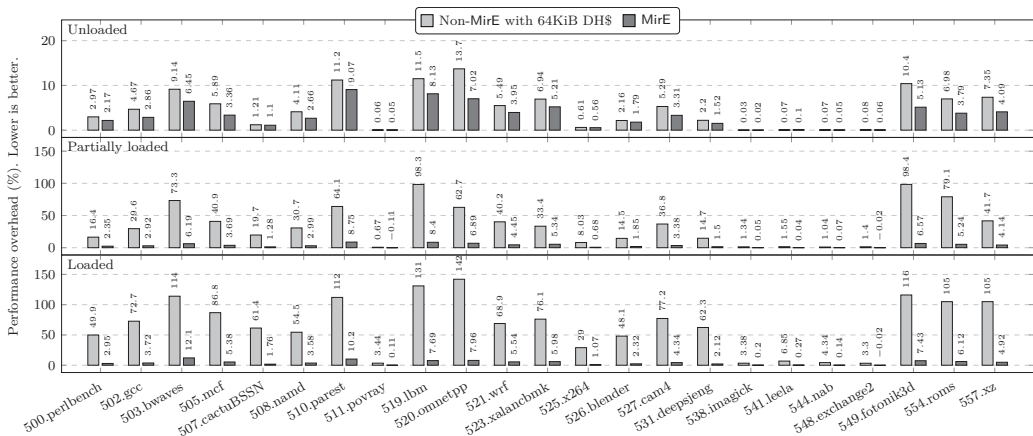


**Figure 15: Set 8** (Section 5.10). L2 impact of MirE when using QARMA: L2/QARMA/32b/CL64B vs. L2/QARMA/MirE/28b/CL64B.

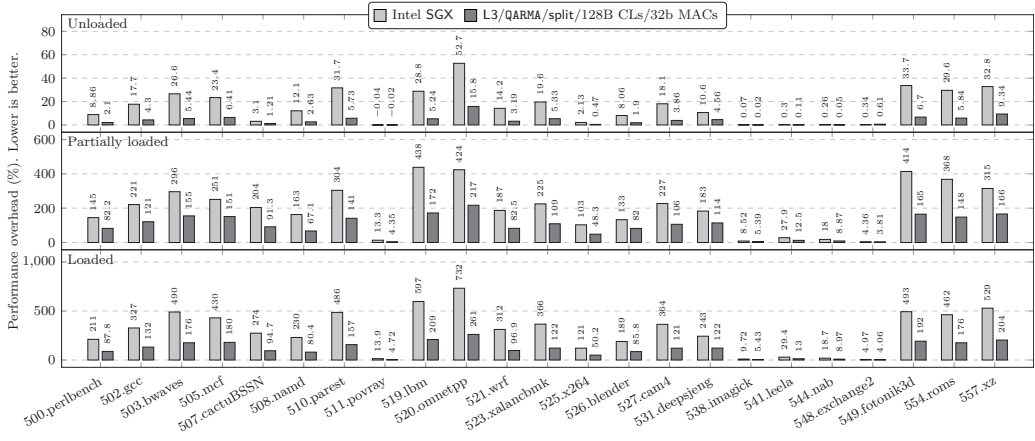


Figure 16: Set 8 (Section 5.10). Impact of split counters: L3/AES/mono-8/56b/CL64B (Intel SGX) vs. L3/QARMA/split-128/32b/CL128B.

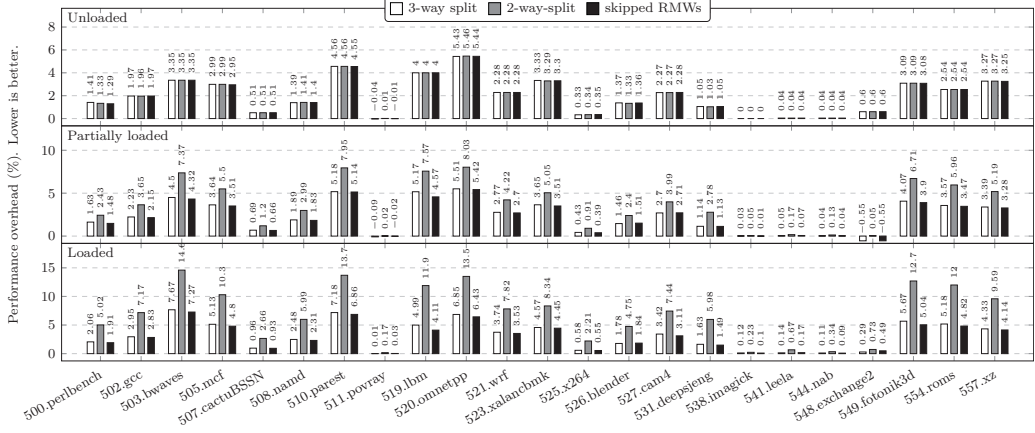


Figure 17: Sets 8 and 9 (Sections 5.10 and 5.11). L3/QARMA/MirE/split-128/LoC/28b/CL128B with 3-way and 2-way split counters, and without RMWs.

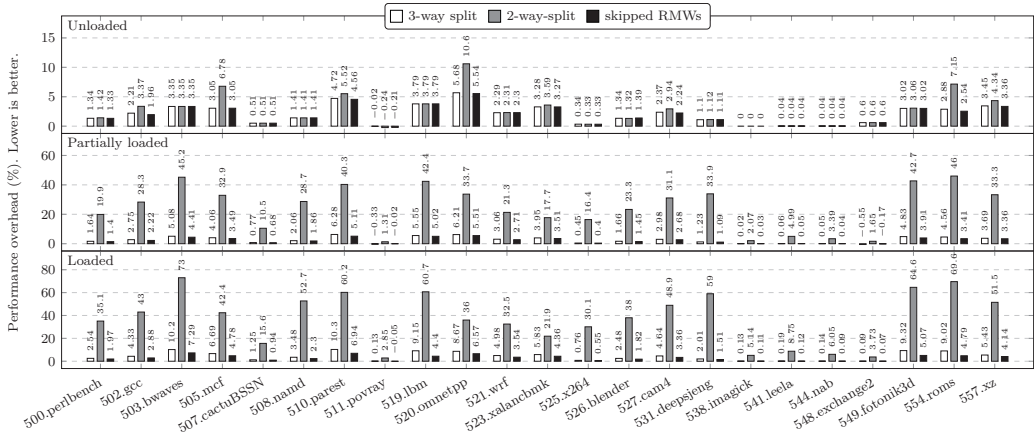


Figure 18: Sets 8 and 9 (Sections 5.10 and 5.11). L3/QARMA/MirE/split-256/LoC/28b/CL128B with 3-way and 2-way split counters, and without RMWs.

also, that a pipelined QARMA circuit and a fully parallelized AES circuit would have comparable total latency — and this would deliver similar performance and security to a L1/L2 scheme, while having different areas.

Integrity can be implemented by re-using the encryption blocks, or by using ad-hoc, smaller ones like QARMA<sub>5-64- $\sigma_0$</sub> , as in [JLK<sup>+</sup>23].

*Remark 2.* Unlike normal CPU caches, the speed of the MPE caches is not critical: counters and hashes just need to be available to the MPE before the data from RAM. This implies that, instead of SRAM, slower DRAM with a much smaller area can be used for these caches.

A DRAM memory cell uses a capacitor and transistor, or in some cases two transistors. The area can thus be capped by two transistors per bit, with a minor amount of control logic. A 4 KiB cache is thus about 64 KGE, and a 256 KiB cache is roughly 4 MGE.

With these numbers at hand, we see that, for modern SoCs with billions of transistors, a single large MPE per memory channel is a small but not negligible cost. Although an additional 1:128 or 1:256 of in-package or in-module DRAM might seem a minor cost, when compared to the total system memory, it cannot be disregarded, especially considering the added expenses of tamper-averting designs. Architects and implementers must weigh all the trade-offs.

## 6 Conclusions

We performed a thorough survey and evaluation of the available technologies for the cryptographic protection of memory contents, together with some previously not considered variants. The numerous possible configurations have each their performance penalty, memory overhead, and hardware cost. The lack of an absolute metric to combine these three costs into one rating makes it very challenging to provide recommendations for each use case. This said, we have enough data to provide some rough guidance.

If only confidentiality is needed, L1 schemes can perform very efficiently, and we recommend the use of a lightweight, high-security encryption primitive (e.g., QARMA) in a direct mode. If integrity protection is required, but replay attacks are out of scope, L2 schemes with a short MAC can be made very efficient by using ECC bits to store the MACs.

Now, let us focus on L3 schemes: nearly-transparent strong memory protection is possible with current technology, but the hardware costs may be prohibitive.

Server SoCs are expensive, with multiple cores and memory channels. Current systems can address a few terabytes of physical memory. The high total system costs allow us to make an argument for counter-based encryption with high arity counter groups stored in on-chip DRAM. The additional cost for counter group storage would be *relatively* minor (1:128 or 1:256 of the external memory). We observe that placing, say, 64 GiB or more of DRAM in a module close to the main SoC is feasible for client devices today. The same technology could be used to place a large tamper-averting memory in a server SoC package, to be used as a large counter cache. When combined with MirE, it would enable the highest level of memory protection at a lower performance impact than all currently deployed schemes without replay protection.

It can be argued that the area budget for such a large memory should rather be used for a system cache, which benefits the *whole* system and reduces the traffic routed through the MPE. Such a cache could also be dynamically re-partitioned between system and MPE. This would rely on an analysis of the traffic and of the impact of the partitioning that goes beyond the scope of this paper.

If these approaches are not possible, storing the integrity tree off-chip and using MirE still provides good performance when combined with a large counter cache.

On client devices, memories usually lack ECC, making MirE not applicable. However, for use cases such as security modules and business oriented containers, memory bus

saturation is less of a concern. We thus expect performance penalties to be contained, usually in line with unloaded systems, and we recommend the use of high arity split counter trees in a dynamically allocated carve-out.

Future work includes contributing our MPE model to the `gem5` project which we hope will stimulate future research and enable studies for specific workloads and configurations.

## Acknowledgments

Parts of Ionuț Mihalcea’s work for this paper was performed in fulfillment of the requirements for an M.Sc. degree [Mih22]. Ionuț wishes to thank his academic supervisor Prof. Konstantinos Markantonakis, and his line manager at Arm, Paul Howard, for their steady support.

David Schall’s work was done during two internships at Arm Research and Arm’s Architecture and Technology Group. Part of the work performed during the first internship is documented in his Master’s Thesis [Sch19].

The authors wish to thank Matthias Boettcher, Mike Campbell, Siddhartha Chhabra, Yuval Elad, Wendy Elsasser, Charles Garcia-Tobin, Alexander Klimov, Kazuhiko Mine-matsu, Jason Parker, Prakash Ramrakhiani, Gururaj Saileshwar, Andrew Swaine, Peter Williams, and Nicholas Wood for many useful discussions.

## References

- [ABD<sup>+</sup>23] Roberto Avanzi, Subhadeep Banik, Orr Dunkelman, Maria Eichlseder, Shibam Ghosh, Marcel Nageler, and Francesco Regazzoni. The QARMAv2 family of tweakable block ciphers. *IACR Transactions on Symmetric Cryptology*, (3):25–73, Sep. 2023. doi:10.46586/tosc.v2023.i3.25-73.
- [AMD20a] AMD. AMD SEV-SNP: Strengthening VM isolation with integrity protection and more, January 2020. Technical Report.
- [AMD20b] AMD. Secure Encrypted Virtualization API Version 0.24, April 2020. Technical Report.
- [AN17] Shaizeen Aga and Satish Narayanasamy. InvisiMem: Smart Memory Defenses for Memory Bus Side Channel. In *Proceedings of ISCA 2017*, pages 94–106, 2017. doi:10.1145/3079856.3080232.
- [App20] Apple Inc. Secure Enclave, 2020. URL: <https://support.apple.com/en-gb/guide/security/sec59b0b31ff/web>.
- [Ava17] Roberto Avanzi. The QARMA Block Cipher Family – Almost MDS Matrices over Rings with Zero Divisors, Nearly Symmetric Even-Mansour Constructions with Non-Involutory Central Rounds, and Search Heuristics for Low-Latency S-Boxes. *IACR Trans. on Symmetric Cryptology*, 2017(1):4–44, 2017. doi:10.13154/tosc.v2017.i1.4-44.
- [Bac14] Matt Bach. ECC and REG ECC Memory Performance, May 2014. URL: <https://www.pugetsystems.com/labs/articles/ECC-and-REG-ECC-Memory-Performance-560/>.
- [BBB<sup>+</sup>11] Nathan L. Binkert, Bradford M. Beckmann, Gabriel Black, Steven K. Reinhardt, Ali G. Saidi, Arkaprava Basu, Joel Hestness, Derek Hower, Tushar Krishna, Somayeh Sardashti, Rathijit Sen, Korey Sewell, Muhammad Shoaib Bin Altaf, Nilay Vaish, Mark D. Hill, and David A. Wood.

- The gem5 Simulator. *SIGARCH Comput. Archit. News*, 39(2):1–7, 2011. doi:[10.1145/2024716.2024718](https://doi.org/10.1145/2024716.2024718).
- [BCG<sup>+</sup>12] Julia Borghoff, Anne Canteaut, Tim Güneysu, Elif Bilge Kavun, Miroslav Knezevic, Lars R. Knudsen, Gregor Leander, Ventzislav Nikov, Christof Paar, Christian Rechberger, Peter Rombouts, Søren S. Thomsen, and Tolga Yalçın. PRINCE — A Low-Latency Block Cipher for Pervasive Computing Applications - Extended Abstract. In *ASIACRYPT 2012*, pages 208–225, 2012. doi:[10.1007/978-3-642-34961-4\\_14](https://doi.org/10.1007/978-3-642-34961-4_14).
- [BJK<sup>+</sup>16] Christof Beierle, Jérémy Jean, Stefan Kölbl, Gregor Leander, Amir Moradi, Thomas Peyrin, Yu Sasaki, Pascal Sasdrich, and Siang Meng Sim. The SKINNY family of block ciphers and its low-latency variant MANTIS. In *Proceedings of CRYPTO 2016, Part II*, pages 123–153, 2016. doi:[10.1007/978-3-662-53008-5\\_5](https://doi.org/10.1007/978-3-662-53008-5_5).
- [Blo70] Burton H. Bloom. Space/time trade-offs in hash coding with allowable errors. *Commun. ACM*, 13(7):422–426, 1970. doi:[10.1145/362686.362692](https://doi.org/10.1145/362686.362692).
- [BLvK18] James Bucek, Klaus-Dieter Lange, and Jóakim von Kistowski. SPEC CPU2017: Next-Generation Compute Benchmark. In *Companion of the 2018 ACM/SPEC ICPE*, pages 41–42. ACM, 2018. doi:[10.1145/3185768.3185771](https://doi.org/10.1145/3185768.3185771).
- [CL10] David Champagne and Ruby B. Lee. Scalable architectural support for trusted software. In *Proceedings of HPCA 2010*, pages 1–12, 2010. doi:[10.1109/HPCA.2010.5416657](https://doi.org/10.1109/HPCA.2010.5416657).
- [CW79] Larry Carter and Mark N. Wegman. Universal Classes of Hash Functions. *J. Comput. Syst. Sci.*, 18(2):143–154, 1979. doi:[10.1016/0022-0000\(79\)90044-8](https://doi.org/10.1016/0022-0000(79)90044-8).
- [CXL19] CXL Consortium. Compute express link™ resource library, 2019. URL: <https://www.computeexpresslink.org/resource-library>.
- [CZG<sup>+</sup>15] Patrick Colp, Jiawen Zhang, James Gleeson, Sahil Suneja, Eyal de Lara, Himanshu Raj, Stefan Saroiu, and Alec Wolman. Protecting data on smartphones and tablets from memory attacks. In *Proceedings of ASPLOS 2015*, pages 177–189. ACM, 2015. doi:[10.1145/2694344.2694380](https://doi.org/10.1145/2694344.2694380).
- [DEMS21] Christoph Dobraunig, Maria Eichlseder, Florian Mendel, and Martin Schläpfer. Ascon v1.2: Lightweight authenticated encryption and hashing. *J. Cryptol.*, 34(3):33, 2021. doi:[10.1007/s00145-021-09398-9](https://doi.org/10.1007/s00145-021-09398-9).
- [DR02] Joan Daemen and Vincent Rijmen. AES and the Wide Trail Design Strategy. In *Proceedings of EUROCRYPT 2002*, pages 108–109, 2002. doi:[10.1007/3-540-46035-7\\_7](https://doi.org/10.1007/3-540-46035-7_7).
- [ECG<sup>+</sup>09] Reouven Elbaz, David Champagne, Catherine H. Gebotys, Ruby B. Lee, Nachiketh R. Potlapally, and Lionel Torres. Hardware mechanisms for memory authentication: A survey of existing techniques and engines. *Trans. Computational Science*, 4:1–22, 2009. doi:[10.1007/978-3-642-01004-0\\_1](https://doi.org/10.1007/978-3-642-01004-0_1).
- [ECL<sup>+</sup>07] Reouven Elbaz, David Champagne, Ruby B. Lee, Lionel Torres, Gilles Sas-satelli, and Pierre Guillemin. TEC-Tree: A Low-Cost, Parallelizable Tree for Efficient Defense Against Memory Replay Attacks. In *Proceedings of CHES 2007*, pages 289–302, 2007. doi:[10.1007/978-3-540-74735-2\\_20](https://doi.org/10.1007/978-3-540-74735-2_20).

- [EEO<sup>+</sup>14] Dmitry Evtvyushkin, Jesse Elwell, Meltem Ozsoy, Dmitry V. Ponomarev, Nael B. Abu-Ghazaleh, and Ryan Riley. Iso-x: A flexible architecture for hardware-managed isolated execution. In *47th Annual IEEE/ACM International Symposium on Microarchitecture, MICRO 2014, Cambridge, United Kingdom, December 13-17, 2014*, pages 190–202, 2014. doi:10.1109/MICRO.2014.25.
- [FAKM14] Bin Fan, David G. Andersen, Michael Kaminsky, and Michael Mitzenmacher. Cuckoo filter: Practically better than bloom. In Aruna Seneviratne, Christophe Diot, Jim Kurose, Augustin Chaintreau, and Luigi Rizzo, editors, *Proceedings of the 10th ACM International on Conference on emerging Networking Experiments and Technologies, CoNEXT 2014, Sydney, Australia, December 2-5, 2014*, pages 75–88. ACM, 2014. doi:10.1145/2674005.2674994.
- [FLD<sup>+</sup>21] Erhu Feng, Xu Lu, Dong Du, Bicheng Yang, Xueqiang Jiang, Yubin Xia, Binyu Zang, and Haibo Chen. Scalable memory protection in the PENGLAI enclave. In *15th USENIX OSDI, July 14-16, 2021*, pages 275–294. USENIX Association, 2021. URL: <https://www.usenix.org/conference/osdi21/presentation/feng>.
- [GJMN16] Robert Granger, Philipp Jovanovic, Bart Mennink, and Samuel Neves. Improved masking for tweakable blockciphers with applications to authenticated encryption. In *Proceedings of EUROCRYPT 2016, Part I*, volume 9665 of LNCS, pages 263–293. Springer, 2016. doi:10.1007/978-3-662-49890-3\_11.
- [GMD<sup>+</sup>16] Johannes Götzfried, Tilo Müller, Gabor Drescher, Stefan Nürnberger, and Michael Backes. Ramcrypt: Kernel-based address space encryption for user-mode processes. In *Proceedings of AsiaCCS 2016*, pages 919–924. ACM, 2016. doi:10.1145/2897845.2897924.
- [Gol87] Oded Goldreich. Towards a theory of software protection and simulation by oblivious rams. In *Proceedings of STOC, 1987*, pages 182–194. ACM, 1987. doi:10.1145/28395.28416.
- [GSC<sup>+</sup>03] Blaise Gassend, G. Edward Suh, Dwaine E. Clarke, Marten van Dijk, and Srinivas Devadas. Caches and Hash Trees for Efficient Memory Integrity Verification. In *Proceedings of HPCA '03*, pages 295–306, 2003. doi:10.1109/HPCA.2003.1183547.
- [Gue16a] Shay Gueron. A Memory Encryption Engine Suitable for General Purpose Processors. *IACR Cryptol. ePrint Arch.*, 2016. URL: <http://eprint.iacr.org/2016/204>.
- [Gue16b] Shay Gueron. Memory Encryption for General-Purpose Processors. *IEEE Secur. Priv.*, 14(6):54–62, 2016. doi:10.1109/MSP.2016.124.
- [HJ05] William Eric Hall and Charanjit S. Jutla. Parallelizable Authentication Trees. In *Proceedings of SAC 2005*, pages 95–109, 2005. doi:10.1007/11693383\_7.
- [HJ08] William E. Hall and Charanjit S. Jutla. US Patent US US7451310 B2: Parallelizable authentication tree for random access storage, filed Dec. 2, 2002. <http://www.google.com/patents/US7451310>, November 2008.

- [HS10] Ruirui C. Huang and G. Edward Suh. IVEC: Off-Chip Memory Integrity Protection for Both Security and Reliability. In *Proceedings of ISCA 2010*, pages 395–406. ACM, 2010. doi:10.1145/1815961.1816015.
- [HSH<sup>+</sup>09] J. Alex Halderman, Seth D. Schoen, Nadia Heninger, William Clarkson, William Paul, Joseph A. Calandrino, Ariel J. Feldman, Jacob Appelbaum, and Edward W. Felten. Lest we remember: cold-boot attacks on encryption keys. *Commun. ACM*, 52(5):91–98, 2009. doi:10.1145/1506409.1506429.
- [HT13] Michael Henson and Stephen Taylor. Memory Encryption: A Survey of Existing Techniques. *ACM Comput. Surv.*, 46(4):53:1–53:26, 2013. doi:10.1145/2566673.
- [IBM99] IBM. Enhancing IBM Netfinity Server Reliability: IBM Chipkill Memory, 1999.
- [IEE19] IEEE. IEEE standard for cryptographic protection of data on block-oriented storage devices 1619–2018, January 2019. URL: <http://ieeexplore.ieee.org/servlet/opac?punumber=4493431>.
- [IK03] Tetsu Iwata and Kaoru Kurosawa. OMAC: One-Key CBC MAC. In *FSE 2003, Revised Papers*, volume 2887 of *LNCS*, pages 129–153. Springer, 2003. doi:10.1007/978-3-540-39887-5\_11.
- [IMO<sup>+</sup>22] Akiko Inoue, Kazuhiko Minematsu, Maya Oda, Rei Ueno, and Naofumi Homma. ELM: A Low-Latency and Scalable Memory Encryption Scheme. *IEEE Trans. Inf. Forensics Secur.*, 17:2628–2643, 2022. doi:10.1109/TIFS.2022.3188146.
- [Int21] Intel. Intel<sup>®</sup> Trust Domain Extensions White Paper, August 2021. URL: <https://www.intel.com/content/www/us/en/developer/articles/technical/intel-trust-domain-extensions.html>.
- [JACH11] Seongwook Jin, Jeongseob Ahn, Sanghoon Cha, and Jaehyuk Huh. Architectural support for secure virtualization under a vulnerable hypervisor. In *44rd Annual IEEE/ACM International Symposium on Microarchitecture, MICRO 2011, Porto Alegre, Brazil, December 3-7, 2011*, pages 272–283, 2011. doi:10.1145/2155620.2155652.
- [JLK<sup>+</sup>23] Jonas Juffinger, Lukas Lamster, Andreas Kogler, Moritz Lipp, Maria Eichlseder, and Daniel Gruss. CSI:Rowhammer – Cryptographic Security and Integrity against Rowhammer. In *Proceedings of IEEE S&P '23*, 2023.
- [JMSS20] Simon Johnson, Raghunandan Makaram, Amy Santoni, and Vinnie Scarlata. Supporting Intel<sup>®</sup> SGX on multi-socket platforms, August 2020. Technical Report.
- [JNRV20] Samuel Jaques, Michael Naehrig, Martin Roetteler, and Fernando Viridia. Implementing Grover Oracles for Quantum Key Search on AES and LowMC. In *Proceedings of EUROCRYPT 2020, Part II*, volume 12106 of *LNCS*, pages 280–310. Springer, 2020. doi:10.1007/978-3-030-45724-2\_10.
- [Kel02] John Kelsey. Compression and Information Leakage of Plaintext. In *Proceedings of FSE 2002*, volume 2365 of *LNCS*, pages 263–276. Springer, 2002. doi:10.1007/3-540-45661-9\_21.

- [KLR<sup>+</sup>20] Mohamed Amine Khelif, Jordane Lorandel, Olivier Romain, Matthieu Regnery, Denis Baheux, and Guillaume Barbu. Toward a hardware Man-in-the-Middle attack on PCIe bus. *Microprocess. Microsystems*, 77, 2020. doi:10.1016/j.micpro.2020.103198.
- [KPW16] David Kaplan, Jeremy Powell, and Tom Woller. AMD Memory Encryption White Paper, April 2016. URL: <https://www.amd.com/system/files/TechDocs/memory-encryption-white-paper.pdf>.
- [LAA<sup>+</sup>20] Jason Lowe-Power, Abdul Mutaal Ahmad, Ayaz Akram, Mohammad Alian, Rico Amslinger, Matteo Andreozzi, Adrià Armejach, Nils Asmussen, Srikant Bharadwaj, Gabe Black, Gedare Bloom, Bobby R. Bruce, Daniel Rodrigues Carvalho, Jerónimo Castrillón, Lizhong Chen, Nicolas Derumigny, Stephan Diestelhorst, Wendy Elsasser, Marjan Fariborz, Amin Farmahini Farahani, Pouya Fotouhi, Ryan Gambord, Jayneel Gandhi, Dibakar Gope, Thomas Grass, Bagus Hanindhito, Andreas Hansson, Swapnil Haria, Austin Harris, Timothy Hayes, Adrian Herrera, Matthew Horsnell, Syed Ali Raza Jafri, Radhika Jagtap, Hanhwi Jang, Reiley Jeyapaul, Timothy M. Jones, Matthias Jung, Subash Kannoth, Hamidreza Khaleghzadeh, Yuetsu Kodama, Tushar Krishna, Tommaso Marinelli, Christian Menard, Andrea Mondelli, Tiago Mück, Omar Naji, Krishnendra Nathella, Hoa Nguyen, Nikos Nikoleris, Lena E. Olson, Marc S. Orr, Binh Pham, Pablo Prieto, Trivikram Reddy, Alec Roelke, Mahyar Samani, Andreas Sandberg, Javier Setoain, Boris Shingarov, Matthew D. Sinclair, Tuan Ta, Rahul Thakur, Giacomo Travaglini, Michael Upton, Nilay Vaish, Ilias Vougioukas, Zhengrong Wang, Norbert Wehn, Christian Weis, David A. Wood, Hongil Yoon, and Éder F. Zulian. The gem5 Simulator: Version 20.0+. *CoRR*, abs/2007.03152, 2020. arXiv:2007.03152, doi:10.48550/arXiv.2007.03152.
- [LKS<sup>+</sup>20] Dayeol Lee, David Kohlbrenner, Shweta Shinde, Krste Asanovic, and Dawn Song. Keystone: an open framework for architecting trusted execution environments. In *Proceedings of EuroSys '20*, pages 38:1–38:16. ACM, 2020. doi:10.1145/3342195.3387532.
- [LMMR21] Gregor Leander, Thorben Moos, Amir Moradi, and Shahram Rasoolzadeh. The SPEEDY family of block ciphers engineering an ultra low-latency cipher from gate level for secure processor architectures. *IACR Trans. Cryptogr. Hardw. Embed. Syst.*, 2021(4):510–545, 2021. doi:10.46586/tches.v2021.i4.510-545.
- [MAB<sup>+</sup>13] Frank McKeen, Ilya Alexandrovich, Alex Berenzon, Carlos V. Rozas, Hisham Shafi, Vedvyas Shanbhogue, and Uday R. Savagaonkar. Innovative instructions and software model for isolated execution. In *Proceedings of HASP 2013*, page 10, 2013. doi:10.1145/2487726.2488368.
- [Mer80] Ralph C. Merkle. Protocols for Public Key Cryptosystems. In *Proceedings of the 1980 IEEE S&P*, pages 122–134, 1980. doi:10.1109/SP.1980.10006.
- [Mih22] Ionuț Mihalcea. Prototyping Memory Integrity Tree Algorithms for Internet of Things Devices. Master’s thesis, Information Security Group, Royal Holloway University of London, UK, 2022.
- [MMS<sup>+</sup>20] Tsutomu Matsumoto, Ryo Miyachi, Junichi Sakamoto, Manami Suzuki, Dai Watanabe, and Naoki Yoshida. RAM encryption mechanism without hardware support. *J. Inf. Process.*, 28:473–480, 2020. doi:10.2197/ipsjjip.28.473.

- [MPS<sup>+</sup>21] Dominic P. Mulligan, Gustavo Petri, Nick Spinale, Gareth Stockwell, and Hugo J. M. Vincent. Confidential Computing - a brave new world. In *Proceedings of SEED 2021*, pages 132–138. IEEE, 2021. doi:10.1109/SEED51797.2021.00025.
- [MZLS18] Saeid Mofrad, Fengwei Zhang, Shiyong Lu, and Weidong Shi. A comparison study of intel SGX and AMD memory encryption technology. In *Proceedings of the 7th International HASP@ISCA 2018 Workshop, Los Angeles, CA, USA, June 02-02, 2018*, pages 9:1–9:8. ACM, 2018. doi:10.1145/3214292.3214301.
- [NHSQ12] Yao Nianmin, Ma Haifeng, Cai Shaobin, and Han Qilong. A memory integrity protection method based on Bloom filter. In *11th International Symposium on Distributed Computing and Applications to Business, Engineering and Science*, pages 305–309, 2012. doi:10.1109/DCABES.2012.101.
- [NIS12] NIST. FIPS PUB 180-4 – Secure Hash Standard. Technical report, National Institute of Standards and Technology, Gaithersburg, MD, United States, March 2012. URL: <https://csrc.nist.gov/publications/detail/fips/180/4/final>.
- [NIS15] NIST. FIPS PUB 202 – SHA-3 Standard: Permutation-Based Hash and Extendable-Output Functions. Technical report, National Institute of Standards and Technology, Gaithersburg, MD, United States, August 2015. URL: <https://csrc.nist.gov/publications/detail/fips/202/final>.
- [Pet10] Peter A. H. Peterson. Cryptkeeper: Improving security with encrypted RAM. In *Proceedings of IEEE HST 2010*, pages 120–126, 2010. doi:10.1109/THS.2010.5655081.
- [RCPS07] Brian Rogers, Siddhartha Chhabra, Milos Prvulovic, and Yan Solihin. Using Address Independent Seed Encryption and Bonsai Merkle Trees to Make Secure Processors OS- and Performance-Friendly. In *Proceedings of MICRO-40, 2007*, pages 183–196, 2007. doi:10.1109/MICRO.2007.44.
- [Rog04] Phillip Rogaway. Efficient Instantiations of Tweakable Blockciphers and Refinements to Modes OCB and PMAC. In *ASIACRYPT 2004, Proceedings*, pages 16–31, 2004. doi:10.1007/978-3-540-30539-2\_2.
- [SA21] Omais Shafi and Ismi Abidi. CuckoOnsai: An efficient memory authentication using amalgam of cuckoo filters and integrity trees. In *58th ACM/IEEE Design Automation Conference, DAC 2021, San Francisco, CA, USA, December 5-9, 2021*, pages 1273–1278. IEEE, 2021. doi:10.1109/DAC18074.2021.9586205.
- [San14] Andreas Sandberg. *Understanding Multicore Performance: Efficient Memory System Modeling and Simulation*. PhD thesis, Uppsala University, Disciplinary Domain of Science and Technology, Mathematics and Computer Science, Department of Information Technology, Division of Computer Systems, Uppsala, Sweden, 2014.
- [SBS<sup>+</sup>21] Martin Schwarzl, Pietro Borrello, Gururaj Saileshwar, Hanna Müller, Michael Schwarz, and Daniel Gruss. Practical Timing Side Channel Attacks on Memory Compression. *CoRR*, abs/2111.08404, 2021. arXiv:2111.08404, doi:10.48550/arXiv.2111.08404.

- [SCG<sup>+</sup>03a] G. Edward Suh, Dwaine E. Clarke, Blaise Gassend, Marten van Dijk, and Srinivas Devadas. AEGIS: architecture for tamper-evident and tamper-resistant processing. In *Proceedings of ICS 2003*, pages 160–171, 2003. doi:[10.1145/782814.782838](https://doi.org/10.1145/782814.782838).
- [SCG<sup>+</sup>03b] G. Edward Suh, Dwaine E. Clarke, Blaise Gassend, Marten van Dijk, and Srinivas Devadas. Efficient Memory Integrity Verification and Encryption for Secure Processors. In *Proceedings of the 36th Annual International Symposium on Microarchitecture*, pages 339–350, 2003. doi:[10.1109/MICRO.2003.1253207](https://doi.org/10.1109/MICRO.2003.1253207).
- [Sch19] David H. Schall. Evaluation and Optimization of Memory Encryption and Integrity Protection. Master’s thesis, University of Kaiserslautern, Department of Electrical Engineering and Information Technology, Microelectronic Systems Design Research Group, 2019.
- [Shw15] Shweta Shinde and Shruti Tople and Deepak Kathayat and Prateek Saxena. PodArch: Protecting Legacy Applications with a Purely Hardware TCB. Technical Report NUS-SL-TR-15-01, School of Computing, National University of Singapore, February 2015.
- [Sko17] Sergei Skorobogatov. How microprobing can attack encrypted memory. In *Proceedings of DSD 2017*, pages 244–251. IEEE Computer Society, 2017. doi:[10.1109/DSD.2017.69](https://doi.org/10.1109/DSD.2017.69).
- [SL12] Jakub Szefer and Ruby B. Lee. Architectural support for hypervisor-secure virtualization. In *Proceedings of the 17th ASPLOS, 2012*, pages 437–450. ACM, 2012. doi:[10.1145/2150976.2151022](https://doi.org/10.1145/2150976.2151022).
- [SMS<sup>+</sup>22] Moritz Schneider, Ramya Jayaram Masti, Shweta Shinde, Srdjan Capkun, and Ronald Perez. Sok: Hardware-supported trusted execution environments. *CoRR*, abs/2205.12742, 2022. arXiv:[2205.12742](https://arxiv.org/abs/2205.12742), doi:[10.48550/arXiv.2205.12742](https://doi.org/10.48550/arXiv.2205.12742).
- [SNOT21] Kuniyasu Suzuki, Kenta Nakajima, Tsukasa Oi, and Akira Tsukamoto. TS-Perf: General Performance Measurement of Trusted Execution Environment and Rich Execution Environment on Intel SGX, Arm TrustZone, and RISC-V Keystone. *IEEE Access*, 9:133520–133530, 2021. doi:[10.1109/ACCESS.2021.3112202](https://doi.org/10.1109/ACCESS.2021.3112202).
- [SNR<sup>+</sup>18a] Gururaj Saileshwar, Prashant J. Nair, Prakash Ramrakhyani, Wendy El-sasser, José A. Joao, and Moinuddin K. Qureshi. Morphable Counters: Enabling Compact Integrity Trees For Low-Overhead Secure Memories. In *Proceedings of the 50th IEEE/ACM MICRO, 2018*, pages 416–427. IEEE Computer Society, 2018. doi:[10.1109/MICRO.2018.00041](https://doi.org/10.1109/MICRO.2018.00041).
- [SNR<sup>+</sup>18b] Gururaj Saileshwar, Prashant J. Nair, Prakash Ramrakhyani, Wendy El-sasser, and Moinuddin K. Qureshi. SYNERGY: Rethinking Secure-Memory Design for Error-Correcting Memories. In *Proceedings of HPCA 2018*, pages 454–465. IEEE Computer Society, 2018. doi:[10.1109/HPCA.2018.00046](https://doi.org/10.1109/HPCA.2018.00046).
- [SPHC02] Timothy Sherwood, Erez Perelman, Greg Hamerly, and Brad Calder. Automatically Characterizing Large Scale Program Behavior. In *ACM SIGPLAN Notices, vol. 37 (Proceedings of ASPLOS-X, 2002)*, pages 45–57. ACM Press, 2002. doi:[10.1145/605397.605403](https://doi.org/10.1145/605397.605403).

- [TBC<sup>+</sup>20] Meysam Taassori, Rajeev Balasubramonian, Siddhartha Chhabra, Alaa R. Alameldeen, Manjula Peddireddy, Rajat Agarwal, and Ryan Stutsman. Compact leakage-free support for integrity and reliability. In *Proceedings of the 47th ISCA*, pages 735–748. IEEE, 2020. doi:10.1109/ISCA45697.2020.00066.
- [TJ09] Randy Torrance and Dick James. The State-of-the-Art in IC Reverse Engineering. In *Proceedings of CHES 2009*, volume 5747 of *LNCS*, pages 363–381. Springer, 2009. doi:10.1007/978-3-642-04138-9\_26.
- [TSB18] Meysam Taassori, Ali Shafiee, and Rajeev Balasubramonian. VAULT: Reducing Paging Overheads in SGX with Efficient Integrity Verification Structures. In *Proceedings of ASPLOS 2018*, pages 665–678. ACM, 2018. doi:10.1145/3173162.3177155.
- [UHM<sup>+</sup>20] Rei Ueno, Naofumi Homma, Sumio Morioka, Noriyuki Miura, Kohei Matsuda, Makoto Nagata, Shivam Bhasin, Yves Mathieu, Tarik Graba, and Jean-Luc Danger. High Throughput/Gate AES Hardware Architectures Based on Datapath Compression. *IEEE Trans. Computers*, 69(4):534–548, 2020. doi:10.1109/TC.2019.2957355.
- [WB11] Peter Williams and Rick Boivie. CPU support for secure executables. In *Trust and Trustworthy Computing - 4th International Conference, TRUST 2011. Proceedings*, pages 172–187, 2011. doi:10.1007/978-3-642-21599-5\_13.
- [WWB<sup>+</sup>19] Samuel Weiser, Mario Werner, Ferdinand Brasser, Maja Malenko, Stefan Mangard, and Ahmad-Reza Sadeghi. TIMBER-V: tag-isolated memory bringing fine-grained enclaves to RISC-V. In *Proceedings of the 26th NDSS 2019*. The Internet Society, 2019. URL: [https://www.ndss-symposium.org/wp-content/uploads/2019/02/ndss2019\\_10-3\\_Weiser\\_paper.pdf](https://www.ndss-symposium.org/wp-content/uploads/2019/02/ndss2019_10-3_Weiser_paper.pdf).
- [YA18] Salessawi Ferede Yitbarek and Todd M. Austin. Reducing the Overhead of Authenticated Memory Encryption Using Delta Encoding and ECC Memory. In *Proceedings of DAC 2018*, pages 1–35. ACM, 2018. doi:10.1145/3195970.3196102.
- [YEP<sup>+</sup>06] Chenyu Yan, Daniel Engleder, Milos Prvulovic, Brian Rogers, and Yan Solihin. Improving Cost, Performance, and Security of Memory Encryption and Authentication. In *Proceedings of ISCA 2006*, pages 179–190, 2006. doi:10.1109/ISCA.2006.22.